Final Technical Report
Earthquake Hazards Program

Collaborative Research between the Nevada Bureau of Mines and Geology and the USGS on the Paleoearthquake History of the Kings Canyon Fault Zone, Nevada

Craig M. dePolo

Nevada Bureau of Mines and Geology
University of Nevada, Reno
Reno, Nevada 89557

September 2014

US Geological Survey EHP Award No. G12AP20047

Research supported by the U.S. Geological Survey (USGS), Department of the Interior, under USGS Award Number G12AP20047. The views and conclusions contained in this document are those of the author and should not be interpreted as necessarily representing the official policies, either expressed or implied, of the U.S. Government.

Table of Contents

Abstract ….. **3**
Acknowledgements ….. **3**
Overview ….. **4**
Kings Canyon fault zone ….. **4**
Previous Studies ….. **6**
    Earthquake History Derived from Trexler and Bell (1979a) ….. **7**
2012 Exploratory Trenching ….. **8**
    Trench 1 ….. **8**
    Trench 2 ….. **9**
    Trench 3 ….. **10**
    Stratigraphy of Trenches 1-3 ….. **12**
    Soil Development ….. **16**
Dating of Deposits ….. **16**
Results of the Investigation ….. **18**
    Total Offset of Alluvial Fan Deposits ….. **18**
    Number of Paleosearthquakes ….. **19**
    Ages of Paleoearthquakes ….. **22**
    Displacements of Paleoearthquakes ….. **25**
    Fault Slip Rates and Interseismic Intervals ….. **26**
    Implications for the Earthquake History of the Carson Range fault system ….. **26**
References ….. **27**
Appendix A Soils Report ….. **29**
Appendix B Radicarbon Sample Analysis Report ….. **52**

Plate 1 Trench 1 Log
Plate 2 Trench 2 Log
Plate 3 Trench 3 Log

Abstract

Three trenches and one soil pit were excavated across a major strand of the Kings Canyon fault zone, in western Carson City, Nevada. The site features fault scarps in a compound alluvial fan. Previous studies (Trexler and Bell, 1979a) indicated there was an incipient, but distinct, soil in these deposits that had been offset along the fault zone. The trenches were mapped, units were delineated based on physical characteristics, and 18 samples were collected for AMS radiocarbon and luminescence dating. Trench 3 was across a more northeasterly striking part of the fault that has a relatively simple fault scarp, whereas the other two trenches (Trenches 1 and 2) were placed on the opposite side of a graben. The larger normal dip-slip offsets and simple fault exposed in Trench 3 yielded the best paleoseismic information, with a series of stacked colluvial deposits, each thought to be related to an earthquake event. The results of this study were somewhat surprising. The preferred interpretation of the information collected is that four paleoearthquakes with offsets ~2 m occurred between ~4000 and ~1420 years ago. Alternative three-event and two-event models that fit these time frames are also considered. At Trench 3, a total vertical offset of 8.4 ±0.5 m across the fault was created by these late Holocene events. Dates indicated that the offset alluvial fan surface was much younger than previously thought (~5 ky vs. ~15 ky). Thus, a relatively high slip rate for the Basin and Range Province was calculated for this late Holocene cluster of events. OxCal modeling of the dates and event horizons yielded the following ages and uncertainties for the four-event model:

PE1: 1420 ± 70 cal ybp
PE2: 1630 ± 110 cal ybp
PE3: 1820 ± 140 cal ybp
PE4: 3960 ± 820 cal ybp

The best age for the alluvium just below the fan surface at Trench 3 was KC3-L2 (4420-5260 ybp) and the vertical offset of the fan surface was 8.4 ±0.5 m. This yields a vertical fault slip rate of 1.5 to 2.0 m/ky, but includes two open intervals at either end. Considering the four-event model, three closed intervals can be used to calculate fault slip rate. Considering uncertainties involved, the vertical slip rate of the earthquake cluster PE1-PE3 ranges from 1.7 to 3.9 m/ky. Existing evidence indicates that the Kings Canyon fault zone did not fail during the most-recent event along the Genoa fault to the south, but there are candidate events along the zone that might be time correlative to the penultimate event along the Genoa fault. The dates from the trench also indicate that a moderately well-developed silica-cemented horizon as much as a meter thick has formed in the fan deposits within the last 2000 years, which was mostly a hyper-arid environment in Nevada.

Acknowledgements

This project was a collaborative effort of many individuals, resulting in a well-documented and highly useful data set; many thanks to all. **Rich Briggs** and **Ryan Gold** from the U.S. Geological Survey have been partners and colleagues throughout this project and these results are really "our results." They surveyed the site, helped log the trenches, collected samples, conducted the OxCal age modeling, and helped put the event models together. **Shannon Mahan** of the U.S. Geological Survey ran the luminescence dates and **Tony Crone** of the U.S. Geological Survey assisted in selecting the trench sites, logging the trenches, and with luminescence dating sample collection. **Shaopeng Dong, Alexander Morelan,** and **Eric Hubbard** were part of the trench logging crew and **Shaopeng Dong** and **Jack Hursh** photographed Trenches 1 and 2. Soil descriptions were provided by **Glen Borchardt** and **Gerald Miller**. **Diane** and **Paige dePolo** assisted in cleaning the trenches. Thanks also to Western Nevada College and **Karen Joost** for permission to excavate on their property.

Overview

This investigation focused on determining the recent paleoseismic history of the Kings Canyon fault zone (KCFZ), a major normal fault that crosses through the western part of Nevada's state capitol, Carson City. Three trenches were excavated in western Carson City. The fault zone was exposed in all three trenches and evidence for two to four late Holocene paleoearthquakes was documented. This project was a joint investigation between the Nevada Bureau of Mines and Geology and the U.S. Geological Survey with the goal of improving our understanding of the seismic hazard of Carson City and western Nevada.

Kings Canyon Fault Zone

The Kings Canyon fault zone is approximately 15 km long and is part of the Carson Range fault system, which bounds the eastern side of the Carson Range in western Nevada and eastern California. The fault zone spans the range front between the Genoa fault to the south and the Virginia Range transverse ridge to the north. This transverse ridge is a major discontinuity within the Carson Range fault system. The southern end of the KCFZ is near Highway 50, where the zone appears to intersect with the Genoa fault (c.f., Stewart, 1999) and an east-west fault with prominent geomorphic expression that crosses the Carson Range at that intersection. The main fault of the KCFZ north of this intersection bounds the west side of a ~1.7 km long interior valley within the Carson Range and crosses over a small divide. North of the divide, western splays of the fault zone trend into and along the base of the Carson Range. The most active trace continues to the north along the eastern side of the zone. This main trace widens into a zone with a cross-strike distance of about 800 m that follows the base and lies within the range front along the eastern side of Kings Canyon. North of Kings Canyon the most active fault trace crosses a fan complex emanating from Ash, Vicee, and Combs Canyon. The trenches excavated during this research were in the southern part of this fan complex, along the most active fault trace. The westernmost fault traces of the Kings Canyon fault bound the western part of the fan complex and appear to be continuous with fault traces that bound the small range front in southern Washoe Valley to the north; these are the faults that break through the Virginia Range transverse ridge. North of the fan complex, the most active and easternmost fault trace of the KCFZ becomes northeast striking, bounds the southeastern side of the Virginia Range a short distance before trending up into the range and towards a Pleistocene volcanic center at McClellan Peak.

The southern intersection with the Genoa fault and the northern ends at the Virginia Range transverse ridge and near McClellan Peak are the most obvious structural discontinuities along the Kings Canyon fault that might be considered earthquake rupture segmentation points. Because faults that cross through the Virginia Range transverse ridge are continuous for kilometers to the north and south of this ridge, this is considered a potentially leaky discontinuity, and earthquake ruptures may rupture through this discontinuity, but perhaps not along the most active trace of the Kings Canyon fault. Similarly the southern intersection has relatively conservative slip and ruptures may cross between the Genoa fault and the KCFZ.

The Virginia Range transverse ridge is a minimum in the total displacement of the Carson Range fault system. Bedrock at the ridge has been displaced about half as much as the total

displacement across the range front fault to the north and south (Ramelli and others, 1999). This smaller amount of total displacement can be achieved by having minimums in adjacent coseismic surface displacements, by not rupturing during all the earthquakes that occur, by having younger displacements, or a combination of these factors. In addition to this displacement minimum, there is a 2.8 km left step in the range front and the range bounding faults on the northern side of the transverse ridge. The transverse ridge is clearly breeched by Quaternary faults, some of which are continuous through the ridge as mentioned. In addition to these, a compound graben has formed at the range front over about ¾ of the ridge's intersection with the range front. Displacements per event on faults that go through the transverse ridge would be instructive to the behavior of faults through this feature. Because of the step in the range front, the fault system may have been structurally integrated later than activity along the main faults. Faults that cross through the transverse ridge are not perfectly aligned with the main range front faults to the north or south, and may have independent earthquake failures as well as potentially rupturing during adjacent range front events.

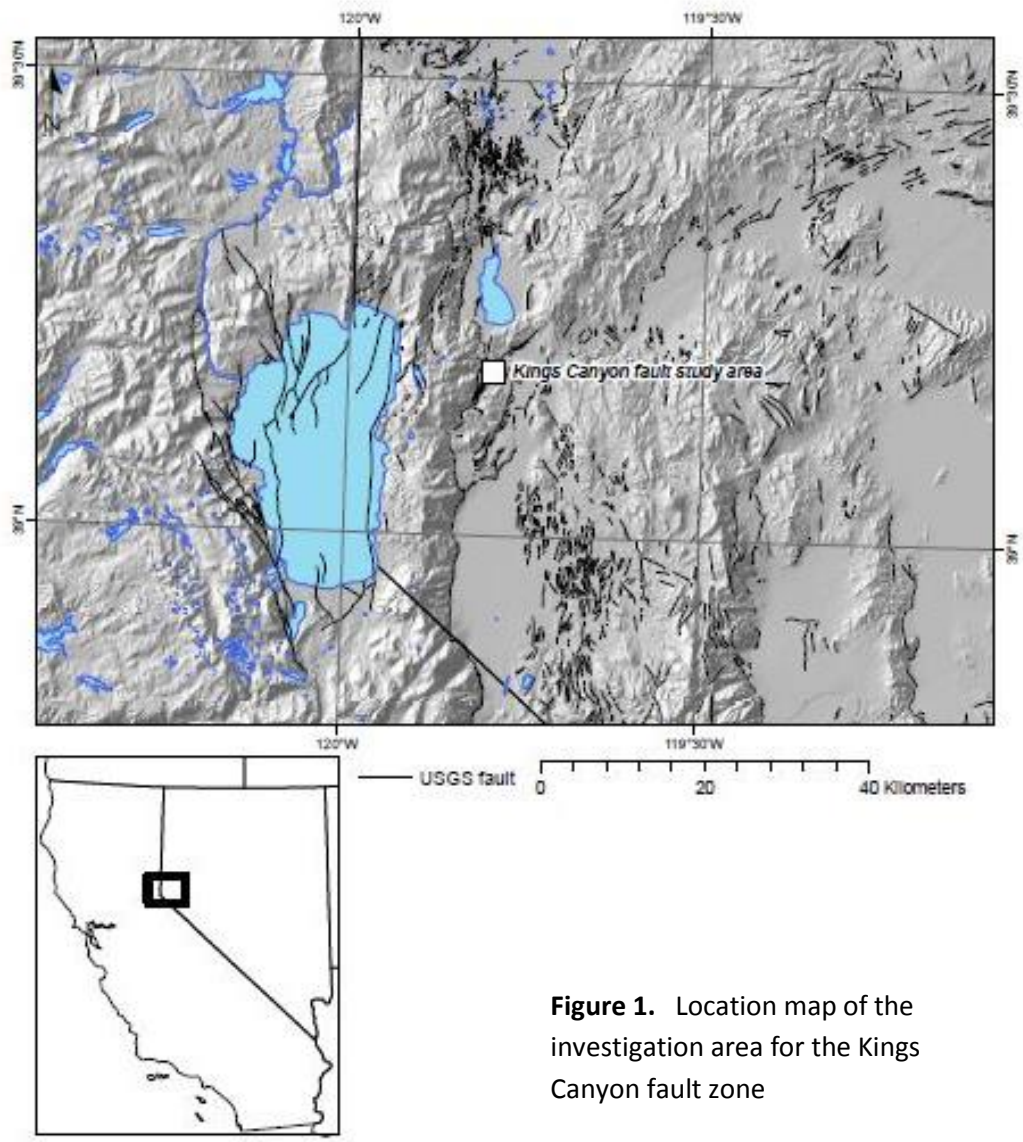

Figure 1. Location map of the investigation area for the Kings Canyon fault zone

Previous Studies

The Kings Canyon fault zone was mapped at a scale of 1:24,000 by Trexler and Bell (1979b), who identified several fault traces with Holocene activity. These fault traces have been used in the U.S. Geological Survey's Quaternary Fault and Fold Database.

Previous trenching at the site was conducted in November 1978 by Dennis Trexler and John Bell from the Nevada Bureau of Mines and Geology (Trexler and Bell, 1979a and 1980), who concluded that at least two Holocene events had occurred along the Kings Canyon fault zone. Trexler and Bell (1979a) excavated four trenches across fault traces that form a 150-m-wide graben in fan deposits in the central part of the Kings Canyon fault zone. Trench 1 (fig. 2) crossed the western side of the graben and Trench 2 (fig. 3) crossed the antithetic scarp on the east side. The paleoseismic history is developed from these two trenches. Trenches 3 and 4 were across the northern extensions the same faults, and although they exposed some additional details, they do not add to the event history. Trexler and Bell (1979a) identified "two movements" in Trenches 1 and 2, which are discussed in more detail in the earthquake history section. The ages of these events were inferred from soils and cross-cutting relationships and qualitative observations of scarp degradation. Trexler and Bell (1979a) identified a haploxerollic soil (a colored cambic soil, sensu latos) overlying a bouldery gravelly alluvial fan deposit. The soil is estimated to be Holocene age, about 5,000 to 12,000 ybp (Trexler and Bell, 1979a and Bell and Trexler, 1980).

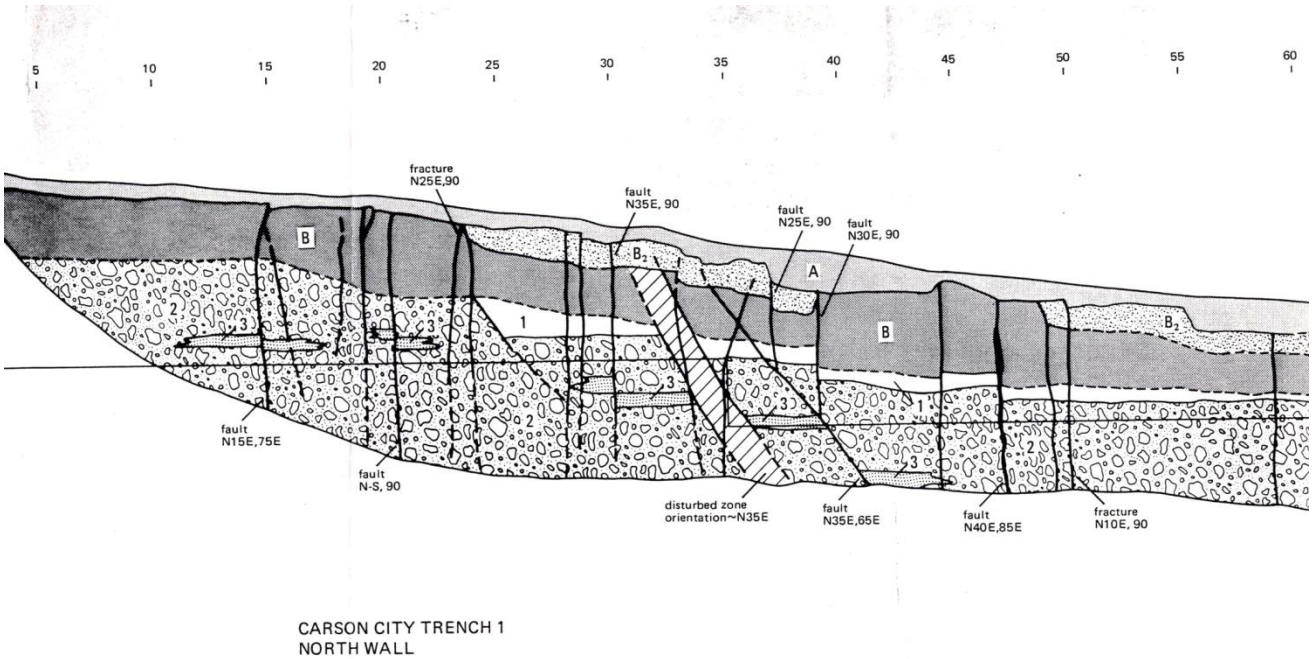

Figure 2. Western part of the Trench 1 log from Trexler and Bell (1979a). In both trench logs: A is a light brownish gray, structureless sandy loam A soil horizon; B is a Typic Haploxeroll (~cambic) horizon in a sandy loam; unit 1 is a medium-gray to light red-brown cobbly sandy gravel (poorly sorted, poorly consolidated, and poorly stratified); unit 2 is a light- to medium-gray bouldery gravel that locally contains stratified sand lenses, and is dominantly made up of decomposed granite; unit 3 is a light-gray medium sand lens, 15-30 cm thick; it is well sorted and moderately to well stratified.

Trench 1 (fig. 2) has an unfaulted A horizon, overlying a fractured and faulted deposit with a haploxerollic soil in it (units B & B2). Below this is a thin deposit (unit 1), which has been down-faulted into the bouldery gravelly grus and was subsequently offset.

Trench 2 (fig. 3) has a fault zone and fractures that cross the A horizon, in addition to fractured deposits with a B horizon similar to Trench 1 (Trexler and Bell, 1979a). The fault zone is near the base of a small, 30-cm-high back-facing fault scarp and the B horizon appears to be down-dropped a similar amount as the surface proximal to this fault zone. Across the main fault, unit 2 deposits are down-faulted and unit 1 deposits within the graben are buttressed and faulted against the main fault. The main fault zone is made up of a widening upwards disturbed zone that offsets the B horizon and a small fault zone in the upper eastern part that is formed in the A and B horizons.

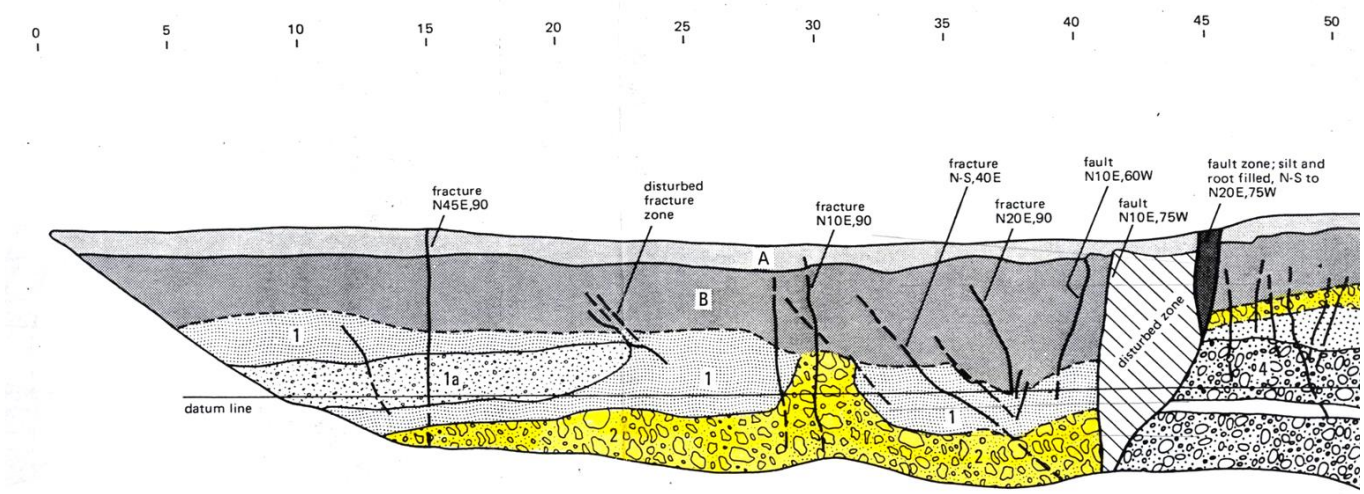

Figure 3. Western part of the Trench 2 log from Trexler and Bell (1979a). See Trench 1 log caption for unit descriptions. In addition to these, unit 1a is a light- to medium-gray to light-brown bouldery gravel lens within unit 1; unit 4 is a light- to medium-gray to light brown sandy, bouldery gravel dominated by grus, with a pebble sand layer (white) within it. Unit 2 is colored yellow.

Earthquake History Derived from Trexler and Bell (1979a)

Paleoearthquakes are named with "Paleoearthquake 1" being the youngest, or the most recent event, and increasing numbers being successively older events. There appears to be evidence for at least three earthquakes in the trench logs from Trexler and Bell (1979a) and they identified at least two events in their report.

T&B79 Paleoearthquake 1

Evidence for the most recent event includes a young scarplet at Trench 2 and the fault zone formed in the A horizon (Trexler and Bell, 1979a; fig.3). Trexler and Bell (1979a) inferred that this scarp was latest Holocene because it appeared fresh and was formed in easily eroded disintegrated granite deposits (grus). Trexler and Bell (1979b) showed this young offset in two locations along the Kings Canyon fault zone and suggested it was possibly <300 ybp.

T&B79 Paleoearthquake 2

Paleoearthquake 2 created the large disturbed zone in the B horizon in Trench 2 and several small factures and offsets of the B horizon in Trenches 1 and 2. This event was estimated to be mid- to late Holocene because it offset the haploxerollic soil identified in the trench (Trexler and Bell, 1979a). Many fractures also are shown as crossing the B horizon and it is interesting to note that some of these are more easterly striking than the fault.

T&B79 Paleoearthquake 3

Below the B horizon in Trench 1 is a pebbly sand (unit 1) that was down-faulted about 45 cm vertically into the underlying deposits (unit 2), but the base of the haploxerollic soil is not shown as being displaced along this fault strand. This offset appears to be older than the movement along other fault strands that offset the base of this soil. The offset of unit 1 is evidence for a third paleoearthquake. Unit 1 was not exposed outside of the graben in the trenches indicating that it was either deposited in a preexisting graben or was preserved by the down-faulting that occurred during Paleoearthquake 3. Paleoearthquake 3 was older than the formation of the haploxerollic soil identified by Trexler and Bell (1979a).

T&B79 Paleoearthquake 4

In Trench 1 there are offsets of unit 3 at stations 30 and 40 that appear to be crossed by the younger unit 1 without offset, indicating these offsets are older than unit 1. Additionally, unit 1 appears to be confined to the graben in Trench 2, which may support a space-creating event prior to unit 1. This is the oldest possible event in the exposed deposits.

2012 Exploratory Trenching

Trench 1

Trench 1 was excavated on the western side of the north-northeast striking graben in the Vicee Canyon fan complex. The scarp along the western fault of the graben is recognizable, but subtle, in the field. It is visible on low-sun-angle aerial photography, however, and was confirmed to be a fault trace by Trexler and Bell (1979a; their Trench 1). In the area of Trench 1, the fault appears to be made up of small faults separated by small ramps. The down-to-the-east fault scarp that was trenched has a strike of 18° and an apparent vertical surface offset of 40 cm, but it does not coincide with an identified fault and is a little over 2 m to the east of the main fault (F1). Trench 1 was 45 m long, had a maximum depth of a little over 3 m, and was oriented 280°.

Trench 1 (Plate 1) exposed four surface deposits overlying alluvial fan deposits and a fault zone in the vicinity of the fault scarp. Three of these faults are close together and likely intersect a little below the trench exposer (F1a, F1, and F2). Only one fault (F1) had distinct offsets along it and another (F2) had possible offsets and possible repeated fissure open during the youngest events (PE1 and PE2). The other faults were distinguished primarily on the basis of shear fabric observed in units 3 and/or 4 and tended to have overlying, fissure-like downward intrusions of unit 1. Some of the possible fissures in Trench 1 may be related to bending-moment stresses created by downward warping to the

east during recent events. Juxtaposition of different thicknesses of units 3 and 4(?) across fault F1 may be related to a strike-slip component of displacement during recent events.

Trench 2

Trench 2 was excavated across a 30-cm-high N10°E back-facing scarp on the eastern side of the north-northeast striking graben. This fault trace also was also trenched by Trexler and Bell (1979a; their Trench 2). Trench 2 was 30 m long and as much as 3 m deep, and was oriented 275°.

Trench 2 (Plate 2) exposed the subsurface expression of the eastern part of the graben, exposing four distinct units overlying down-dropped fan alluvium to the west of the fault within the graben and three units overlying the fan deposits in the footwall. A well-developed fault (F1) is near the lower part of the fault scarp. This fault formed a buried scarp that was buried by unit 4 and offsets unit 3. A few fractures also were found in the hanging wall. The upper part of fault 1 appears to have a formed a flower structure and the fractures in the hanging wall are potentially part of a flower structure as well.

Trench 3

Trench 3 was excavated in the lower half of a southeast-facing, 7.5-m-high compound fault scarp, striking 65-70°. At the trench site, the scarp has a 3.5-m-high oversteepened base, and 10° and 5° beveled slopes above that. The fault scarp is formed on the front of a small fan remnant that has a small section of relict surface with a 4° slope. A soil pit was placed in this surface. Trench 3 was excavated across the lower half of the fault scarp, centered on the oversteepened base. The trench was >41 m long, as much as 3.5 m deep, and was oriented 335°.

Trench 3 (Plate 3) exposed alluvial fan conglomerates, sandy conglomerates, and sandstones, younger, fluvial sandstones and conglomerates, a sequence of scarp-derived colluvial deposits, and slope-mantling colluvial and soil deposits in the hanging wall of the fault. The alluvial fan deposits were also present in the footwall of the fault, covered by a thin mantle of units 1 and 2. The colluvial deposits adjacent to the fault are largely derived from the erosion of fault scarps created during earthquake events. Following the earliest earthquake identified, fluvial sands and gravels were deposited parallel to the fault scarp (unit 4), following this newly created feature in the landscape.

In Trench 3, A distinct, relatively narrow fault was exposed that down--dropped the scarp slope with a normal dip-slip movement during earthquake events. Four scarp-derived colluvial deposits were mapped in the hanging wall, immediately adjacent to the fault, which overly an unconformity on the top of the alluvial fan deposits. This normal fault is tight, meaning it lacks surficial extensional features displayed by other normal faults, such as graben or secondary faults. Only a couple minor fractures were found in the hanging wall.

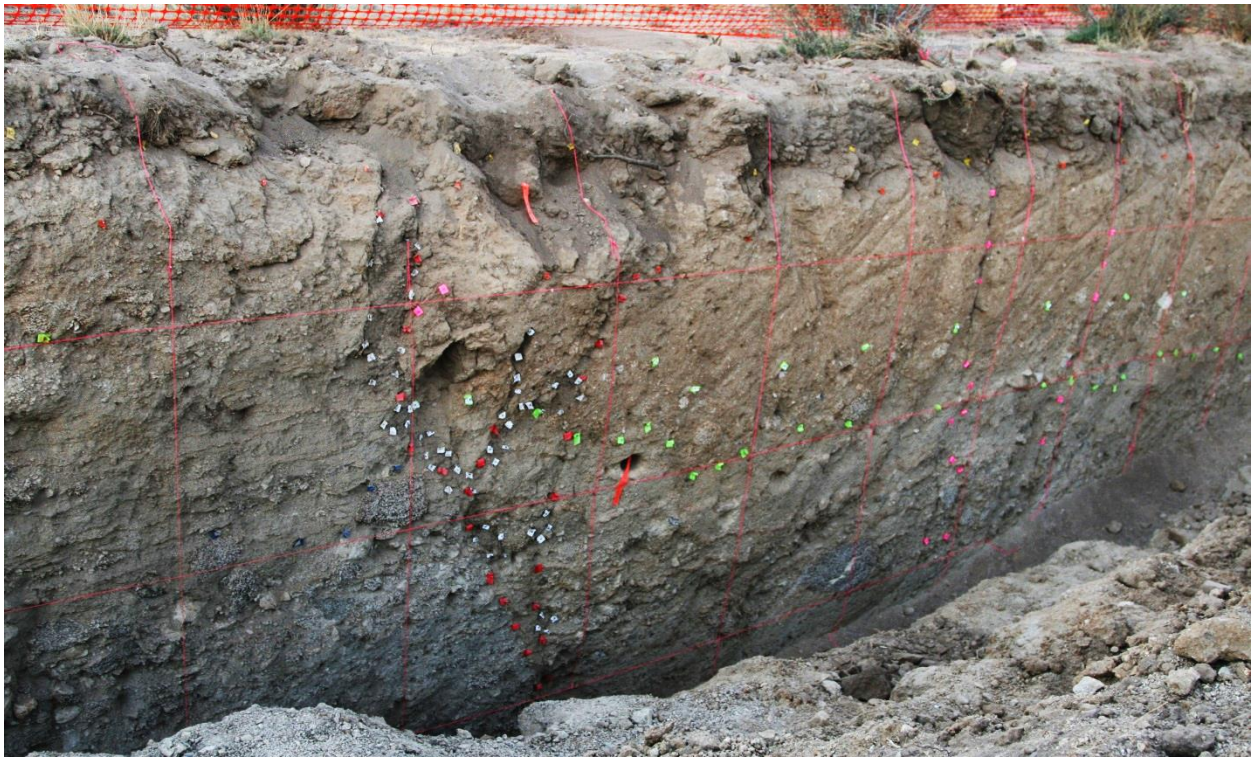

Figure 4. Southern wall of Trench 2 at the fault zone. Graben fill deposits are to the right (west) of the fault zone (red flags).

Figure 5. Fault at Trench 3; view to southwest of the western wall. Colluvial deposits are visible left of the fault. Colluvium 4 is at the base, colluvium 3 is above the lime green flags, colluvium 2 is above the orange flags, and colluvium 1 is in the upper part of the trench wall.

Figure 6. West wall of Trench 3 showing the stacked colluvial deposits left of the fault (red), labeled C1-C4. To the right of the fault are alluvial fan deposits. In the four-event model, each colluvial deposit is a wedge deposit related to an event.

Stratigraphy of Trenches 1, 2, and 3

Five general deposition units were mapped in Trenches 1, 2, and 3, units 1-4 and the alluvial fan deposits. These units are the result of complex surficial processes including fluvial and debris-flow deposition, Colluvial deposition, eolian influx, pedogenesis, and bioturbation. All deposits had some evidence of soil formation, although the soil horizons were only weakly to moderately developed. A soil pit on the more stable fan surface exposed a compound soil in the alluvial fan deposits. Adjacent to the fault, units 1-4 became thicker and were deemed to be colluvial deposits formed dominantly of materials shed from the fault scarp and potentially related to paleoearthquake events. Because of their importance, these were broken out as colluvial deposits with the same numbers as the units they correspond to.

Unit 1

The uppermost soil layer that blankets the site is unit 1, a 10- to 45-cm-thick dark-brown A horizon, that includes significant eolian input. Unit 1 also commonly fills krotovinas and krotovina-modified fissures as deep as 1 m below the surface. Unit 1 is a fine to medium sand with some coarse sand, very coarse sand, and silt. Clasts are generally angular to subangular grains of disintegrated granite, including feldspar, quartz, and biotite, and some organic material including rootlets, plant fragments, wood fragments, and seeds. Soil structure was loose with some weak fine blocky peds. Unit 1 includes about 1% minor gravel and rarer cobbles, which generally appear to be eroded from the underlying alluvium, forming as a lag deposit on the surface.

Unit 2

Unit 2 is a reddish brown very-fine, fine, medium granitic sand, with some coarse sand and silt sized grains and minor rootlets. Clasts in unit 2 are mostly angular and subangular. There are some subrounded clasts, mostly the coarse sand grains. Unit 2 has about 1 to 2% of scattered gravel and rare cobbles. Unit 2 is a 20 to 25 cm thick and has a colored cambic B soil horizon formed in it. This unit appears to be formed from eolian and colluvial deposition. This sandy deposit lies below unit 1 in trench exposures, except where it has been eroded away off the fault scarp formed by the most-recent-event. The lower contact of unit 2 ranges from abrupt and even to irregular and slightly gradational with unit 3.

Unit 2 has medium to large scale platy soil structure and small to medium irregular blocky structure. The color and cohesion exhibited in peds from unit 2 are due to a coating or interstitial filling of fine and very fine sand grains. The peds break down readily in water and there is no reaction with HCl. It also seems possible that weak silica cement may be present; some peds have a vesicular appearance, similar to unit 3 below, which has silica cementation.

Unit 3

Unit 3 is a massive-appearing silica-cemented reddish-brown coarse, fine, medium sand with less than 10% granitic cobbles. Unit 3 is made up of granitic sand that seems to be enriched in quartz relative to the alluvial fan sands. Some quartz grains have a milky white appearance and have secondary deposits in some shattered-looking parts. Additionally a number of biotite grains have been oxidized to a reddish black color. Overall clasts are angular and subangular, with some subrounded grains. Unit 3 has moderate silica cementation (Bq horizon), which was somewhat surprising given the late Holocene age of the deposit. Small vesicles are present, which may be related to fluid movement through the unit and the cementation.

Where it is present, unit 3 is about 0.1 to 1.1 m thick. It was deposited on the hanging wall in Trench 3, and within the graben and as thinner layers on the footwalls in Trenches 1 and 2.

Most parts of unit 3 have relatively few gravel and cobbles, such as in Trenches 1 and 2, but in the central part of Trench 3 there are 5 to 10% cobbles in the lower part of the unit. Unit 3 lacks internal sedimentary structure. The massive, matrix-dominated appearance of unit 3 may indicate that it was deposited as a unit, perhaps as a debris flow. The relative increase in quartz in the sand was likely due to weathering of the material prior to deposition. Dating of colluvial deposit 3 (which was contemporary with unit 3) and

from above and below that deposit, indicates unit 3 was laid down within a short time period of about 300 to 500 years (below unit 3 – KC3-L4 **1.9 ±0.1 ka**; within unit 3 – KC3-L5 **1.7 ±0.1 ka**; above unit 3 – KC3-L6 **1.6 ±0.1 ka**).

Unit 4 and Unit 4(?)

Unit 4 deposits are coarse, fine, medium sands with as much as 25 to 30%, mostly granitic cobbles. Clasts are angular and subangular with some subrounded medium and coarse sized sand grains. The sand composition is similar to the alluvial sands but with a slightly lower percentage of mafic versus felsic minerals. Cobbles are 90% granitic and 10% metavolcanic and metasedimentary rocks. Most of the granitic cobbles are saprolite. Gravel clasts have similar composition makeups. In Trench 3, unit 4 ranges in color from light gray to light gray mottled with brownish and reddish brown patches. In Trenches 1 and 2, the matrix in unit 4(?) was light brown to dark brown

Unit 4 and unit 4(?) are made up of fluvial, colluvial, and/or possible debris deposits that were laid down on the alluvial fan deposits, shortly after the oldest paleoearthquake recognized in the trenches. The unit is defined in Trench 3 and correlated by superposition and character into Trenches 1 and 2, which is why there is a question mark after the "4" in Trenches 1 and 2. Unit 4 deposits are as much as 1.2 m thick in Trench 3 and are present in the hanging walls, but not in the foot walls of Trenches 2 and 3. In Trench 1, unit 4(?) appears as a tapered deposit across the trench that is thickest at its western end and pinches out near the eastern end of the trench. In Trench 3, unit 4 deposits are fluvial with a transport direction that is at a high angle to the trench, parallel to the first fault scarp. Fluvial structures include lenticular and layered beds and cut-and-fill buttress unconformities. These deposits erode into, and possibly interfinger(?) with, colluvial deposit 4. Units 4 and 4(?) contain micro-B horizons that are 1-3 mm thick stringers of Fe-oxide colored clay deposition and are commonly separated by a few cm to 10 cm.

In Trenches 1 and 2, unit 4(?) has fewer fluvial structures and is more massive appearing than unit 4 in Trench 3. Unit 4(?) deposits have matrix-supported gravel and cobble clasts and may have had a colluvial and/or debris-flow origin. In Trench 2, the eastern side of unit 4(?) appears to have been trapped within the graben and deposited against a back-facing fault scarp formed from the earliest event exposed in the trenches.

Alluvial Fan Deposits

Alluvial fan deposits were exposed in the lower part of the trenches and in the soil pit. These are fluvial and debris flow deposits that form the upper part of the alluvial fan complex at the trench site.

The alluvial fan deposits are generally gray cobbly and non-cobbly angular and subangular coarse granitic sands, with some very coarse and medium sand. There were some subrounded very coarse sand grains and cobbles, and a few boulders, as much as 60 cm in diameter. Sedimentary structure varied from thin, regular well-bedded sand layers and lenses to massive cobbly coarse sand layers as much as a half a meter thick. Most clasts were single crystals of disintegrated granitic rock, but the coarser grains were multiple crystal grains, or small pieces of granitic rock. There was a remarkable lack of mechanical weathering of the sand grains, indicating much of the transportation was as debris deposits that were not aggressively tumbling the grains.

Scarp-Derived Colluvial Deposits

In Trench 3, Four colluvial deposits were identified in the hanging wall adjacent to the fault (Plate 3). These four deposits are stacked on top of one another and the entire package is on top[of alluvial fan sediments.

The interpretation that the colluvial deposits in Trench 3 are tectonic colluvial wedges was complicated by the fact that the grusy parent material made relatively indistinct colluvial wedge facies. The few rocks there were that could have formed a proximal facies were commonly chemically weathered into grus prior to being incorporated into the colluvium and disintegrated with erosion, making the deposits massive in nature. The colluvial deposits commonly thickened towards the fault, especially immediately adjacent to the fault, consistent with buttressing against a newly formed scarp (Plate 3).

Colluvial Deposit 1

Colluvium 1 was largely made up of dark brown sandy silt, similar to unit 1. It was a tapered deposit, with a maximum thickness of 60 cm near the fault. Colluvium 1 was deposited in the hanging wall and across the fault as the scarp from the most-recent event eroded back.

Colluvial Deposit 2

Colluvium 2 was 60-cm-thick brown sandy silt with some gravel clasts. The deposit overlies an unconformity on the top of colluvium 3 and includes a moderately well-developed stone line at its base; elsewhere unit 2 (which is at least partly correlative to colluvium 2) has a more gradational lower contact.

The upper contact on colluvium 2 was may have been an unconformity or was relatively conformable; the contact had a somewhat gradation appearance. This may indicate a short amount of time occurred between these two deposits.

Colluvial Deposit 3

Colluvium 3 is made up of brown cemented sands and cobbly sands derived alluvial fan and colluvial deposits. The deposit was massive appearing with some internal slope-oriented gravel clasts. Colluvium 3 was reddened and moderately cemented with silica. Colluvium 3 was deposited on an unconformity on top of colluvium 4 and was sheared against the fault. Colluvium 3 was tabular shaped, but tapered as it approaches the scarp slope. An unconformity formed on the top of colluvium 3 and was subsequently buried by colluvium 2.

Colluvial Deposit 4

The oldest scarp-derived colluvium was at the bottom of the trench adjacent to the fault. Colluvium 4 overlied an unconformity on the alluvial fan deposits that has eroded off the original surface and an unknown amount of the alluvial fan deposits. The colluvium is made up of gray cobbly sandstone in a 1.2-m-thick truncated wedge with little internal sedimentary structure. Colluvium 4 was sheared against the fault and had interfingering(?) and erosional/buttress depositional contacts with fluvial sands and conglomerates adjacent to it in the hanging wall. Granitic clasts in the colluvium were mostly deteriorated and could be disintegrated easily. Colluvium 4 also contained micro-B

horizons that were 1-3 mm thick stringers of Fe-oxide colored clay, commonly separated by a few cm to 10 cm.

Soil Development

A compound soil was found on the best-preserved fan surface consisting from bottom to top, parent material with thin sub-horizontal clay seams, a silica-cemented Bq horizon, a weakly colored Bw horizon, and an organic rich, fine sand A horizon. This is a generalized description and a more in-depth description of the soil by Dr. Glen Borchardt is given in Appendix A. On the slopes and in tectonically disturbed areas these horizons formed within depositional packages. The compound soil appears to have been formed at different times because of the occurrence of unconformities and aggradation within the upper horizons. For example, the thin clay seams in the lower part likely began formation before the sediments in the A, Bw, and Bq horizons were deposited.

The moderate silica-cement in the Bq horizon is of note because it appears to have formed during the last ~2000 years, a remarkably short period of time. A clue to understanding this cementation may come from the climate during this time, which was one of persistent droughts, including century-long droughts (e.g., Mensing and others, 2004).

Dating of Deposits

The exposed deposits in Trench 3 and some deposits in Trench 2 were dated with radiocarbon and optically stimulated luminescence techniques (table 1). Eight radiocarbon samples were collected as bulk samples and all but one were sent to the Paleoresearch Institute to have the organics separated out and identified. For the most organic rich sample, I was able to separate out the organics using a probe, tweezers, and binocular microscope. AMS radiocarbon dating was performed on these organics at the national Ocean Sciences AMS Facility at Woods Hole Oceanographic Institute. Ten luminescence samples, collected by Tony Crone and Ryan Gold, were dated by Shannon Mahan, all from the U.S. Geological Survey. Laboratory errors were remarkably low ranging from 0.6 to 11% of the sample age, with most less than 6%.

The dates collected in this study are presented in Table 1. Most of the dates were from Trench 3, where the evidence of paleoseismic activity was the strongest. In general, the dates was internally consistent and in chronologic order (Plate 3). Two radiocarbon dates were discarded as detrital samples that were too old relative to the other dates (KC2-R1 and KC3-R5) and two micro-charcoal sample dates were discarded because they were dramatically too young and are considered intrusive (KC3-R6 and KC3-R7). Out of the 18 dates collected, 16 were used to constrain the paleoseismic history. Thirteen dates were used by Rich Briggs in an OxCal model for calendar correction of the radiocarbon dates and to constrain the age of the paleoseismic events (presented later in text).

Table 1 Radiocarbon and Luminescence Dates Collected

Trench 2

Sample No.	Unit Dated	Laboratory Age (ybp)	OxCal Age (cal ybp)	Comments
KC2-L1	alluvial fan	5170 ±220		
KC2-L2	alluvial fan	3490 ±400		
KC2-L3	unit 3	1700 ±120		
KC2-R1	unit 3	5540 ±35	6400-6290	detrital

Trench 3

Sample No.	Unit Dated	Raw Lab Age (ybp)	OxCal Age (cal ybp)	Comments
KC3-L1	alluvial fan	5310 ±290	5300 ±300	
KC3-L2	alluvial fan	4840 ±420	4800 ±400	
KC3-L3	unit 4	3120 ±180	3100 ±200	
KC3-L4	colluvium 4	1920 ±60	1900 ±100	
KC3-L5	colluvium 3	1680 ±70	1700 ±100	
KC3-L6	colluvium 2	1660 ±80	1600 ±100	
KC3-L7	colluvium 1	1440 ±50	1400 ±100	
KC3-R1	colluvium 2	1630 ±25	1610-1410	
KC3-R2	colluvium 1	855 ±25	900-690	
KC3-R3	colluvium 1	1550 ±40	1540-1350	
KC3-R4	colluvium 2	1450 ±55	1520-1280	
KC3-R5	colluvium 2	4430 ±40	5280-4870	detrital
KC3-R6	colluvium 4	329 ±22		microcharcoal
KC3-R7	colluvium 3	405 ±24		microcharcoal

Results of the Investigation

Total Offset of the Alluvial Fan Deposits

The total offset of the alluvial fan surface was measured at Trench 3 using an eroded upper original surface (at the Soil Pit 1) and the buried lower original surface of the mid-Holocene fan deposit that was exposed in the trench. The vertical offset across the compound fault scarp was 7.4 m, measured at the mid-point of the fault scarp where the fault was located (fig. 4). In the subsurface there was an additional 1 m of buried offset of the approximate lower original surface (fig. 5). Thus, there was a total of 8.4 m of vertical offset of the mid-Holocene fan surface across the Kings Canyon fault zone. Potential projection errors, unaccounted for burial, and unaccounted for erosion uncertainties are

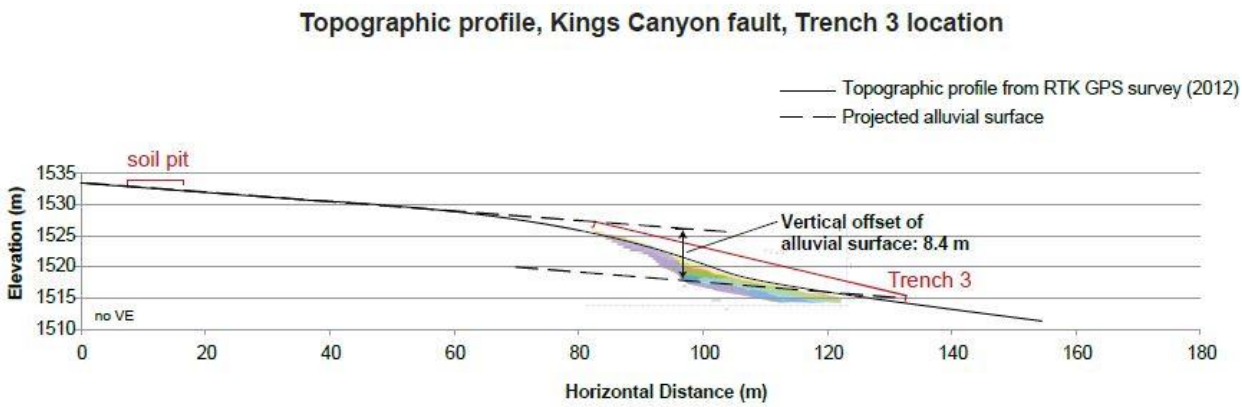

thought to collectively be limited to 0.5 m.

Figure 4 Topographic profile of the Trench 3 site with the Trench 3 log superimposed on it. The location of the trench and the soil pit are shown on the figure. Offset of the alluvial fan surface is shown by the projection lines. The upper projection is a reasonable approximation of the original surface and the lower projection is on a buried alluvial surface.

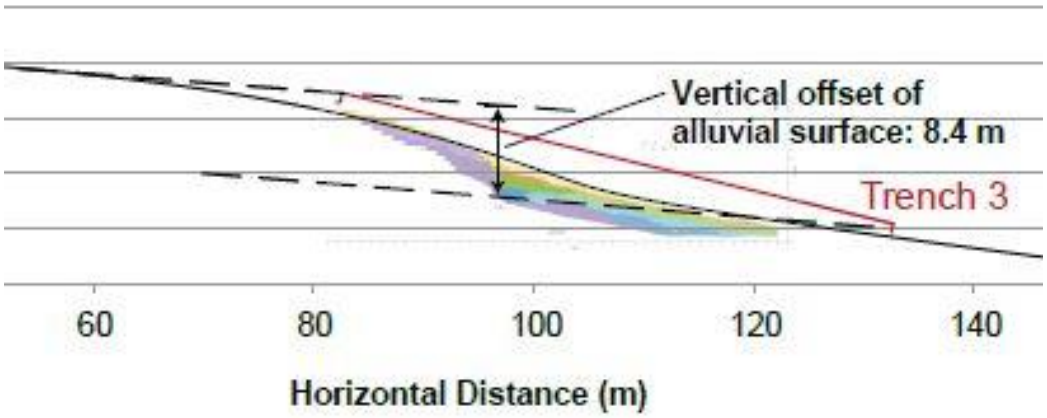

Figure 5 Enlargement of the central part of Figure 4; the fault is where the offset arrows are. The alluvial fan deposits exposed in Trench 3 are purple and are buried on the hanging wall. The upper dashed line is the surface projection and the lower line is this projection on top of the buried alluvial fan deposits, parallel to the upper surface projection. The lower projection indicates about a meter of burial has occurred on the lower surface along the profile. Thus, the total offset of the fan surface is about 8.4 m. Potential projection error, unaccounted for burial, and unaccounted for erosion uncertainties are thought to collectively be limited to 0.5 m.

Number of Paleoearthquakes

Trenching studies along the Kings Canyon fault zone indicate that two to four paleoearthquakes have occurred since mid-Holocene. The principal evidence for these events includes scarp-derived colluvium, offset deposits, radiocarbon and optically-stimulated-luminescence dates, and the youngest fault scarp. The four-event model assumes that each colluvial deposit adjacent to the fault in Trench 3 developed following a paleoearthquake and the collapse and erosion of a related fault scarp. Each of these colluvial deposits appears to be deposited on an unconformity, or paleosurface, and all but the youngest colluvial deposit are buttressed against the fault, increase in thickness towards the fault, and are sheared along the fault. The colluvial deposits lie on a surface that may be back-rotated along the fault.

The dates of the youngest colluvial deposits (1-3) indicate that the sediments were deposited over hundreds of years, including the time represented by the unconformities between them. Thus, if all the colluvial wedges were created by paleoearthquakes, at least two or three of these events would have occurred within hundreds of years of each other. This is a smaller interseismic interval than has been previously recognized along faults in the Basin and Range Province and several alternative event models have been developed to minimize such extraordinary results. Specifically, the ages of colluvial deposits 1-3 range from a little older than 1700 ±100 ybp (KC3-L5) to 1540-1350 cal ybp near the base of colluvial deposit 1 (KC3-R3), a maximum time range of only about 450 years. The three-event model places two events in this time range and the four-event model places three events within it.

Four-Paleoearthquakes Model (4PE)

The four-paleoearthquakes model (4PE) considers that each colluvial deposit found in Trench 3 was deposited following a ground rupturing earthquake at the site. The oldest event in this model, Paleoearthquake 4 (4PE4), was the first to offset the mid-Holocene fan deposits and surface, and created the first fault scarp of the compound scarp that exists today. Following this event, the downthrown side was buried adjacent to the scarp by colluvial deposit 4 (C4) and by fluvial sediments of unit 4 and 4b, deposited parallel to this scarp. Additional evidence for 4PE4 can be found in Trench 2, where unit 4(?) was deposited against a back-facing fault scarp created by the first event to offset the fan surface.

Paleoearthquake 3 (4PE3) offset an eroded and partially buried fault scarp from event 4PE4 and was followed by the formation of colluvial deposit 3 (C3) at the base of the new scarp (and possibly across the fault, although any evidence for this at Trench 3 was eroded away). Unit 3 and deposit C3 are complicated because they coincide with, and are potentially related to, the formation of a silica-cemented soil horizon. This silica soil horizon continues into alluvial fan deposits where the finer-grained unit 3 is not present (e.g., soil pit 1), and where unit 3 is a thin deposit (e.g., the footwall in Trench 2). Colluvial deposit 3, which appears to be deposited contemporaneous with unit 3, is the thickest adjacent to the fault, but approaches this thickness elsewhere on the hanging wall as well. Nevertheless, deposit C3 is buttressed against the fault and possible rotation between its upper and lower contacts indicates that an event occurred between the deposition of C4 and C3. The lower contact between C4 and C3 appears to be rotated down and is at a lower angle than the upper contact between C3 and C2 (which also appears to be rotated down by later events, just not as much). The difference between these two contacts is about 10°, which is distinct. The best explanation for this difference is that the surface on deposit C4

was down dropped along the fault and was warped downwards a little at the fault; this was buried shortly thereafter by deposit C3. The surface on top of deposit C3 was the eroded slope of a degrading fault scarp.

Other potential evidence for 4PE3 is the thicker unit 3 deposits observed in the graben exposed in Trenches 1 and 2 and in Trexler and Bell's (1979a) Trench 2. The uncertainty in this interpretation would principally be a question of how much erosion of unit 3 in the footwall might have occurred and could the thickness of unit 3 have been the same across the fault at one time? The silica-cemented soil associated with unit 3 extends into the alluvial deposits that are immediately below unit 3 in the footwall of Trench 2, which is consistent with a thinner unit 3 deposited on the footwall, and a thicker unit 3 filling a tectonically accentuated graben. If the B horizon of the haploxerollic soil identified in Trexler and Bell (1979a; Trench 2) corresponds with unit 3 and the silica-cemented soil, then a similar difference in thickness can be seen in their trench log, with the graben having a thickened fill or unit 3. In Trench 1, the offset of unit 4(?) and 3 are likely complicated by a strike-slip component causing a justaposition of different thicknesses of these units, but there is an apparent thickness change of unit 3 that could be explained by an event down dropping the graben.

Paleoearthquake 2 (4PE2) down dropped an eroded scarp and C2 was deposited at the base of the new scarp. In Trench 2, unit 3 was down dropped along the fault by 4PE2, and was subsequently buried by colluvial deposit 2. Colluvial deposit 2 has a Bw soil horizon formed in it and was deposited on a moderately distinct surface, delineated by a moderately-well-developed stone line at the base of colluvial deposit 2 in Trench 3.

Paleoearthquake 1 (4PE1) down dropped the base of the eroded compound fault scarp with a vertical offset of about 1.8 m. Deposit C1 was formed at the base of the 4PE1 fault scarp and across the fault as it eroded back. This is the most recent surface rupturing event along the Kings Canyon fault zone and there is a fairly distinct young fault scarp or oversteepened base associated with it. The expression of the young scarp is discontinuous along the fault because of variations in the amount of offset, simple and complex-distributed fault patterns, and possible warping in some places (especially along the western side of the graben). In Trench 1 there was a possible fissure fill in fault F2 that could have formed during 4PE1. A combination of fissuring and animal burrowing made the discernment of event 4PE1 difficult in Trench 2, but several features mapped in Trexler and Bell's (1979) Trench 2 could represent this event. Trexler and Bell (1979a) also mapped a very young fault zone that essentially went to the surface and potentially post-dates 4PE1; this study did not confirm this young offset.

Three-Paleoearthquakes Models (Model 3PE-A and 3PE-B)

There are two three-event models that differ in whether colluvial deposits 2 or 3 are considered as related to an earthquake. In model 3PE-A, colluvial deposit 2 is considered to be related to an earthquake and colluvial deposit 3 is considered to be the upper part of the earlier colluvial package related to the oldest event (3PE3). In model 3PE-B, colluvial deposit 3 is considered to be related to an earthquake and colluvial deposit 2 is the upper part of that colluvial package.

Model 3PE-A considers colluvial deposits 1, 2, and 4 in Trench 3 were related to earthquake displacements. These were the most distinct deposits buttressed against the fault. In the three-event model, Paleoearthquake 3 (3PE3) was the first event to offset the mid-Holocene fan deposits and surface, and created the first fault scarp of the compound

scarp. Following this event, the downthrown side adjacent to the scarp was buried by colluvium (C4 and C3) and by fluvial deposits that were deposited parallel to the scarp. Additional evidence for this event can be found in Trench 2, where unit 4(?) appears to be deposited against a fault scarp, which would have been created by the first event to offset the fan surface. Paleoearthquake 2 (3PE2) similarly down dropped an eroded scarp and C2 was deposited at the base of the new scarp. Event 3PE2 also down dropped unit 3 along the fault in Trench 2; this offset appears to have been subsequently buried by unit 2. Paleoearthquake 1 (3PE1) down dropped an eroded fault scarp and deposit C1 was formed at the base of the 3PE1 scarp, across the fault.

In model 3PE-A, unit 3 and deposit C3 in Trench 3 were deposited on unit 4 without any tectonic activity. These deposits blanketed the hanging wall and whether they extended into the footwall at Trench 3 is not known; there was none present in the footwall exposed in Trench 3, but this was an eroded scarp face.

Model 3PE-B considers colluvial deposits 1, 3, and 4 were related to earthquakes. Paleoearthquake 3 (3PE3) was the first event to offset the mid-Holocene fan deposits and surface, and created the first fault scarp of the compound scarp. Following this event, the downthrown side was buried by colluvium (C4) adjacent to the scarp and fluvial sediments were deposited parallel to the scarp. Additional evidence for this event can be found in Trench 2, where unit 4(?) appears to be deposited against a fault scarp, which would have been from the first event to offset the fan surface. Paleoearthquake 2 (3PE2) offset an eroded fault scarp and was followed by the formation of colluvial deposit 3 at the base of the new scarp. Colluvial deposit 2 would have been deposited on top of colluvial deposit 3. Other potential evidence for 3PE2 is the thicker unit 3 deposits observed in the graben exposed in Trenches 1 and 2 and in Trexler and Bell's Trench 2. Paleoearthquake 1 (3PE1) down dropped an eroded fault scarp and deposit C1 was formed at the base of the 3PE1 scarp, across the fault.

The three-paleoearthquakes models have been informally described as the models of least astonishment. The age of the deposits is such that it only invokes one interseismic interval that is hundreds of years in duration, yet still considers most of the buttressed and down-faulted colluvial deposits next to the fault to be related to ground offsets from earthquakes.

Two-Paleoearthquakes Models (Models 2PE-A and 2PE-B)

It is clear that at least two events have occurred at the trench site. The 7.5-m-high compound fault scarp was formed by all the events, but at its base is a locally-distinct oversteepened base related to the most-recent event, which only accounts for part of the overall scarp. The entire offset from the most-recent event can be viewed in Trench 3. Thus, it is clear that at least two paleoearthquakes created the compound scarp and offset the alluvial fan. Two two-paleoearthquakes models were considered, one based on separating the ages of deposits and one based on having similar displacements for each event. Given the data collected during this study, the two-event model was the only way to obtain an interseismic interval that was a few thousand years versus a couple hundred years in duration. A few thousand years would be a more common interval time for the more active faults in the Basin and Range Province, which the Kings Canyon fault zone clearly is geomorphically and kinematically part of. The most active faults in the Basin and Range Province have slip rates of one to several meters per kiloyear, and thus, kiloyears are required to get offsets of a couple meters or larger. A two-event model using the oldest

event (>~3000 ybp) and an event from the younger package (<~1900 ybp) has an interseismic interval a little over a thousand years.

The difference between the two-event models is the age of the most-recent event. More specifically, did the most-recent event occur immediately prior to the formation of colluvial deposit 2 (model 2PE-A) or did it occur after (perhaps interrupt the formation of) colluvial deposit 2 (model 2PE-B)? In model 2PE-A, colluvial deposits 1-2 were deposited after the most-recent event and in model 2PE-B, only colluvial deposit 1 was deposited after this event. Although it is likely, there is some uncertainty because of rodent burrowing as to whether the backside of unit 2 was faulted by the most recent event. Colluvial deposit 1 crosses the fault, is not offset, and clearly post-dates the most-recent event.

Another difference between these models is the displacement per event. The vertical offset of the most-recent event considering colluvial unit 1 can be fairly precisely measured at 1.8 m (base of C1 to the projection of the offset scarp slope). If C2 is added to this, only the vertical thickness of C2 needs to be added to the C1 offset because the scarp still represents 2PE1 (no older, eroded back scarp from the offset of C2 would have to be considered). Thus, the vertical offset of 2PE1 for model 2PE-A is 2.4 m and from model 2PE-B is 1.8 m. Considering the total vertical offset of 8.4 m and the offsets estimated for 2PE1, event 2PE2 had a much larger displacement than 2PE1, with a vertical offset of 6 m (2PE-A) to 6.6 m (2PE-B). Although not out of the realm of possibilities, that would be an extraordinarily large offset for a 15-km-long fault zone. If this displacement occurred, a linkage with other faults to the south and/or possibly to the north would be suspected.

The two-event models invoke an extraordinary offset for 2PE2 and ignore most of the evidence of paleoearthquake activity from Trench 3. Although these models are plausible, they are considered the less likely explanation for all the information available.

Ages of Paleoearthquakes

The ages of the paleoearthquakes were determined by 11 bracketing luminescence and radiocarbon dating of the sediments and OxCal calendar correction modeling. The dates and uncertainties were put into the OxCal v. 4.2.3 program for calendar correcting and sequencing the dates by Dr. Rich Briggs of the U.S. Geological Survey and the results were used to constrain the ages of the paleoearthquakes (fig 6). The ages of the events are discussed in terms of the four-event model because it has the maximum number of events. Other paleoseismic models use subsets of these events as indicated. The ages of the four paleoearthquakes are given in Table 2.

Paleoearthquake 4PE1, 3PE1, or 2PE-A1

The youngest possible event created a fault scarp with 1.8 m of vertical surface offset at the base of a compound scarp at the Trench 3 site. The younger scarp is visible at the Trench 3 site, but becomes less distinct and is discontinuous elsewhere where vertical offsets were not as large. Colluvial deposit C1 developed across the fault and dates from that unit provide a minimum age for this paleoearthquake. The event offset deposit C2, which along with unit 2, blanketed the Trench 3 site; unit 2 was exposed in the first beveled slope above the youngest basal scarp in the hanging wall (plate 3). The maximum age of the youngest possible event is the age of deposit C2.

The OxCal model age for events 3PE1 and 4PE1 was 1420 ±70 ybp. A minimum age for this event comes from a radiocarbon date near the base of deposit C1 (KC3-R3; 1540-1350 cal ybp) and a luminescence date near the upper part of deposit C1 (KC3-L7; 1500-1300 ybp). The maximum age of the youngest event is constrained by a radiocarbon date from the upper part of deposit C2 (KC3-R1; 1610-1410 cal ybp). There were two other dates from the lower part of deposit C2, which were a luminescence date (KC3-L6; 1700-1500 ybp) and a co-located radiocarbon date (KC3-R4; 1520-1280 cal ybp).

Paleoearthquake 4PE2, 3PE-A2, or 2PE-B1

The second youngest possible event occurred just prior to the deposition of deposit C2 and after deposit C3 was laid down. The down-dropped surface from this event had a moderately-well-developed stone line preserved on it in Trench 3, the best one observed during this investigation. Dates from deposit C2 provide a minimum age for this event and dates from deposit C3 provide a maximum age.

The OxCal model age for event 4PE2 is 1630 ±110 ybp. The minimum age for this event was constrained with two dates from the lower part of deposit C2, a luminescence date (KC3-L6; 1700-1500 ybp) and a co-located radiocarbon date (KC3-R4; 1520-1280 cal ybp). The maximum age of the event was constrained by dates from deposit C3 (KC3-L5; 1800-1600 ybp) and although not used in the OxCal calculation, a date from unit 3 in Trench 2 (KC2-L3; 1820-1580 ybp).

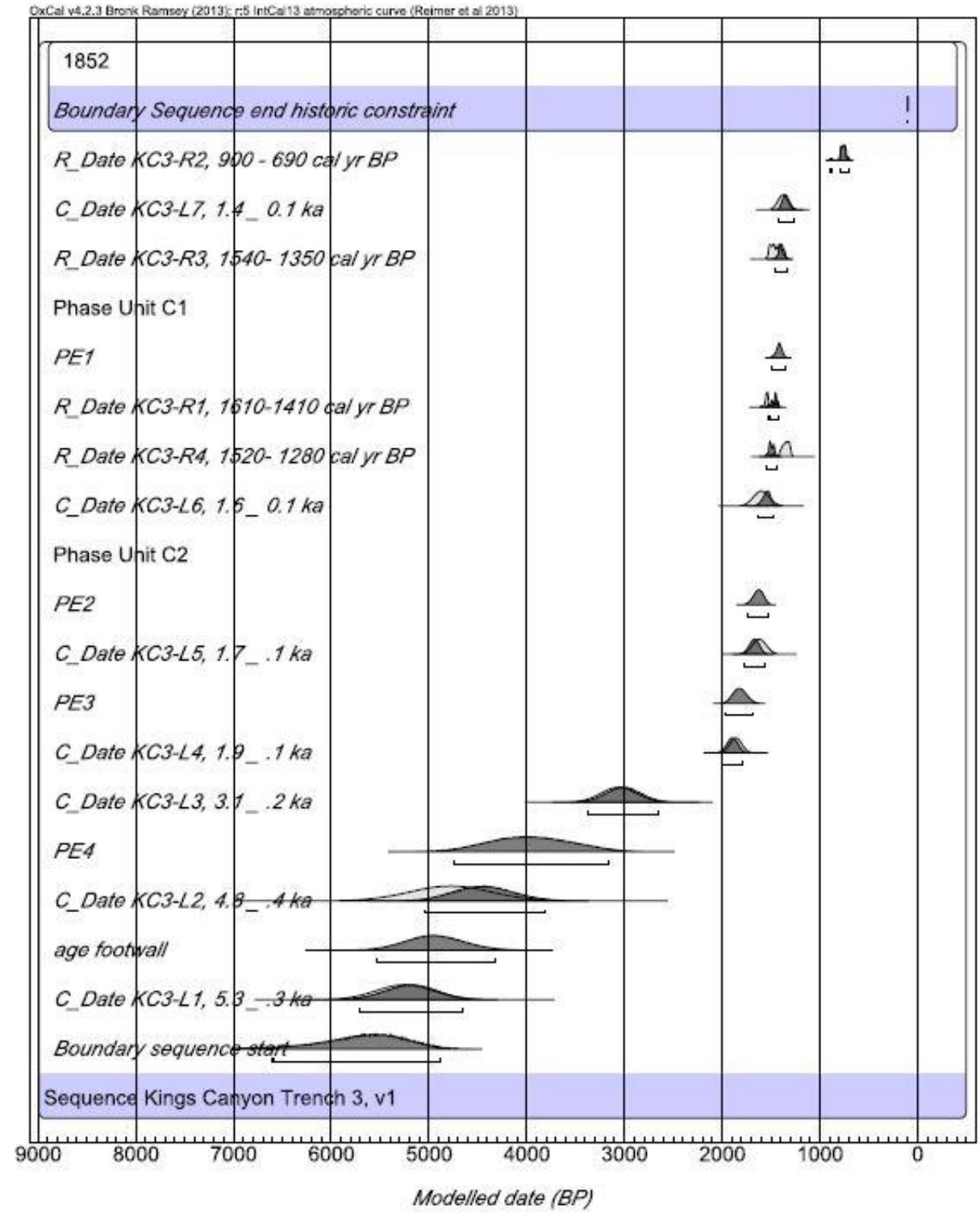

Figure 6. OxCal modeling of the constraining dates and paleoearthquakes (PE1, PE2, PE3, PE4), modeled by Dr. Rich Briggs of the U.S. Geological Survey. The ages of the events are summarized in Table 2.

Paleoearthquake 4PE3 or 3PE-B2

The third possible event back in time occurred just prior to the deposition of deposit C3 and unit 3, and after deposit C4 and unit 4 were laid down. Dates from deposit C3 and unit 3 constrain the minimum age of the event. The surface on deposit C4 and unit 4 were down dropped and dates from these deposits and related deposits constrain the maximum age of the event.

The OxCal model age for event 4PE3 was 1820 ±140 ybp. The minimum age was constrained using dates from deposit C3 (KC3-L5; 1800-1600 ybp) and although not used in the OxCal calculation, a date from unit 3 in Trench 2 (KC2-L3; 1820-1580 ybp). The maximum age constraint comes from a luminescence date from deposit C4 (KC3-L4; 2000-1800 ybp). Additional maximum age constraints from the lower part of unit 4 (KC3-L3; 3300-2900 ybp) and below unit 4(?) in Trench 2 (KC2-L2; 3890-3090 ybp) are at least a 1000 years older.

Paleoearthquake 4PE4,3PE3, or 2PE2

All models use the initial event that offsets the alluvial fan surface and deposits. This event postdates the alluvial fan deposits and predates deposit C4. At Trench 2, unit 4(?) was deposited within the graben and buttressed against a fault scarp from this event.

The OxCal model age for events 4PE4, 2PE2, or 3PE3 was 3960 ±820 ybp. The minimum age comes from a luminescence date from deposit C4 (KC3-L4; 2000-1800 ybp) and from the lower part of unit 4 (KC3-L3; 3300-2900 ybp). The maximum age comes from a luminescence date below the event horizon in the alluvial fan deposits (KC3-L2; 5200-4400 ybp). There is a luminescence date from the fan deposits below unit 4(?) in Trench 2, which appears to have been deposited in the graben following this earliest event; that date would provide a younger constraint that the date at Trench 3 (KC2-L2; 3890-3090 ybp). If this is a valid constraint, the earliest event could have been a few hundred years younger than the OxCal model age.

Table 2. OxCal model ages for the four-paleoearthquake model. The ages for the different subsets of these events in the other multi-event models differ from these ages by no more than 10 years.

PE1: 1420 ± 70 cal ybp
PE2: 1630 ± 110 cal ybp
PE3: 1820 ± 140 cal ybp
PE4: 3960 ± 820 cal ybp

Paleoearthquake Displacements

The total vertical offset of the fan surface of 8.4 m was measured by surveying the compound surface scarp at Trench 3 and estimating the subsurface offset using the log from Trench 3. Possible uncertainties are thought to be less than ±0.5 m.

Modeled vertical surface displacements for the different paleoearthquake models range from 1.8 (measured) to 6.6 m. Considering a total vertical offset of 8.4 m at the trench 3 site, average vertical surface displacements are 2.1 m for the four-event model, 2.8

m for a three-event model, and 4.2 m for a two-event model. The most-recent event had the best preserved vertical offset of all the events because the surface and buried offsets could be measured fairly precisely; these offsets were 1.8 (4PE model) or 2.4 m if colluvial deposits 1 and 2 are both considered to be post-PE1 (2PE-A model). Colluvial deposits 3 and 4 were thicker than colluvium 1 and 2, which may indicate that earlier offsets may have had larger displacements than the two most recent events.

Fault Slip Rates and Interseismic Intervals

The late Holocene fault slip rate for the Kings Canyon fault zone was discovered to be relatively high. This isn't surprising given that an apparent cluster of paleoearthqakes has occurred during this time period along the zone. Two vertical slip rate ranges are calculated, an overall rate using the total fan offset and the age of the alluvial fan surface, and the rate considering three closed interseismic intervals in the four-paleoearthquake model. The best age for the alluvium just below the fan surface at Trench 3 was KC3-L2 (4420-5260 ybp) and the vertical offset of the fan surface was 8.4 ±0.5 m. This yields a vertical slip rate of 1.5 to 2.0 m/ky, but includes two open intervals at either end. The four-paleoearthquake model (and most other models) has closed intervals between the earliest and last events. Thus, the offset from all but the first event and this closed time period a vertical slip rate for the last cluster of three events can be calculated. The offset of PE4 is estimated to be 2 to 2.5 m. This offset was subtracted from the 8.4 m total vertical offset yielding 5.9 to 6.4 m of offset related to the closed interval period. Using the ages of PE1 and PE4 (1420 ±70 and 3960 ±820), the closed time interval is 1650 to 3430 years long. The vertical slip rate of the earthquake cluster (PE1-PE3) ranges from 1.7 to 3.9 m/ky.

Interseismic intervals are calculated as between 190 and 2140 years, using the preferred values from the four-paleoearthquake model. Given age uncertainties are over 50% of the shortest time value and other interseismic intervals can be calculated using other event models, exact values are somewhat suspect. Nevertheless, with exception of the two-event models, all other models produce at least one interseismic interval that is a couple hundred years in duration. The elapsed time since the most-recent event, about 1400 years is longer than all but the interseismic time between PE4 and PE3.

Implications for Earthquake History of the Carson Range Fault System

The information gathered in this study sheds limited light on whether the Kings Canyon fault zone has been a part of ruptures along the Genoa fault to the south or whether it ruptures independently. The two most-recent events along the Genoa fault occurred about 300 ybp and about 1700 ybp (Ramelli and Bell, 2014). A major event was not seen in this trenching study around 300 ybp, and thus a major event along the Kings Canyon fault does not appear to have occurred during the most-recent event on the Genoa fault. A minor faulting event was noted by Trexler and Bell (1979a) in Trench 2 that could be a small offset that was sympathetic or a minor breakage along one strand of the fault during this or another event. It is worth noting that a

Age constraints are not precise enough to rule in or out whether the Kings Canyon fault ruptured with the penultimate event along the Genoa fault. Within the uncertainties, paleoseismic events PE2 or PE3 along the Kings Canyon fault are candidates. If the preferred four-event model is correct, then there are two events along the Kings Canyon

fault zone at about the time of the penultimate event along the Genoa fault. Two similar events have not been recognized along the Genoa fault, thus at least one major, independent event along the Kings Canyon fault would be indicated. The evidence indicates that the Kings Canyon fault zone does not fail with every earthquake along the Genoa fault and likely is involved with earthquakes that are independent from that fault. Unfortunately, whether the Kings Canyon fault zone fails along with some earthquakes along the Genoa fault is not ruled in or out.

An additional consideration is whether or not the Kings Canyon fault zone co-ruptured with the Washoe Valley fault zone to the north, another member of the Carson Range fault system. This is an open question as well because PE2 and PE3 of the Kings Canyon fault zone are similar in age to the maximum age constraint for the penultimate event along the Washoe Valley fault zone (1770 and 1780 ybp; Ramelli and dePolo, 1997). Existing time constraints do not rule out one of the Kings Canyon fault zone pair PE2 and PE3 co-rupturing with the Genoa fault and the other one rupturing with the Washoe Valley fault zone.

A last consideration is the possible co-rupture with the Carson City fault that is in the hanging wall of the Kings Canyon fault zone and parallels it along much of its length. Ramelli and others (1999) collected a piece of charcoal from near the bottom of a fissure formed during PE1 that had a radiocarbon date of 390 ±40 ^{14}C ybp. This a younger event has occurred along the Carson City fault than the Kings Canyon fault zone, which could have been coseismic with the most-recent event along the Genoa fault. The penultimate event along the Carson City fault offset alluvium that had a radiocarbon date of 2,590 ±130 ^{14}C ybp, indicating the event was after 2,348 – 2,953 cal. ybp (using Stuiver and Reimer, 1993 and Reimer and others, 2004). Thus, coseismic rupture of the Kings Canyon fault zone and the Carson City fault during the latest Holocene is not ruled in or out, but the two faults did not rupture together when an event a few hundred years ago occurred along the Carson City fault.

References

Mensing, S.A., Benson, L., Kashgarian, M., and Lund, S., 2004, A Holocene pollen record of persistent droughts from Pyramid Lake, Nevada, USA: Quaternary Research, v. 62, p. 29-38.

Ramelli, A.R. and Bell, J.W., 2014, Spatial and temporal patterns of fault slip rates on the Genoa fault: Nevada Bureau of Mines and Geology Final Technical Report, 19 p.

Ramelli, A.R., Bell, J.W., dePolo, C.M., and Yount, J.C., 1999, Large-magnitude, late Holocene earthquakes along the Genoa fault, west-central Nevada and eastern California: Bulletin of the Seismological Society of America, v. 89, p. 1458-1472.

Ramelli, A.R. and dePolo, C.M., 1997, Trenching and related studies of the northern Sierra Nevada range-front fault system: Nevada Bureau of Mines and Geology, Final Technical Report, U.S. Geological Survey National Earthquake Hazard Reduction Program, contract no. 1434-95-G-2606, 21 p.

Reimer, P. J., Baillie, M. G. L., Bard, E., Bayliss, A., Beck, J. W., Bertrand, C. J. H., Blackwell, P. G., Buck, C. E., Burr, G. S., Cutler, K. B., Damon, P. E., Edwards, R. L., Fairbanks, R. G., Friedrich, M., Guilderson, T. P., Hogg, A. G., Hughen, K. A., Kromer, B., McCormac, F. G., Manning, S. W., Ramsey, C. B., Reimer, R. W., Remmele, S., Southon, J. R., Stuiver, M., Talamo, S., Taylor, F. W., van der Plicht, J., and Weyhenmeyer, C. E., 2004, IntCal04 Terrestrial radiocarbon age calibration, 26 - 0 ka BP: Radiocarbon, v. 46, p. 1029 – 1058.

Stewart, J.H., 1999, Geologic Map of the Carson City 30x60 minute Quadrangle, Nevada: Nevada Bureau of Mines and Geology Map 118, 1:100,000 scale.

Stuiver, M., and Reimer, P. J., 1993, Extended 14C database and revised CALIB radiocarbon calibration program: Radiocarbon, v. 35, p. 215 – 230.

Trexler, D.T. and Bell, J.W., 1979a, Earthquake hazard maps of Carson City, New Empire, and South Lake Tahoe Quadrangles: Nevada Bureau of Mines and Geology Final Technical Report to the U.S. Geological Survey Earthquake Hazard Reduction Program, 43 p.

Trexler, D.T. and Bell, J.W., 1979b, Earthquake hazards of the Carson City Quadrangle: Nevada Bureau of Mines and Geology Map 1Ai, scale 1:24,000.

Appendix A

PEDOCHRONOLOGICAL REPORT FOR THE KINGS CANYON FAULT ZONE, CARSON CITY, CALIFORNIA

Craig dePolo, Reno, NV, NEHRP Project No. G12AP20047

2014-09-09

Soil Tectonics

P.O. Box 5335

Berkeley, CA 94705

Glenn Borchardt

Principal Soil Scientist

Certified Professional Soil Scientist No. 24836

PEDOCHRONOLOGICAL REPORT FOR THE KINGS CANYON FAULT ZONE, CARSON CITY, CALIFORNIA

Craig dePolo, Reno, NV, NEHRP Project No. G12AP20047

2014-09-09

Glenn Borchardt

INTRODUCTION

An assessment of seismic and landslide risk due to ground movement can be aided greatly by the techniques of pedochronology (Borchardt, 1992, 1998), soil dating. This is because the youngest geological unit overlying fault traces and landslide features is generally a soil horizon. The age and relative activity of ground movement often can be estimated by evaluating the age and relative disturbance of overlying soil units.

Soil horizons exhibit a wide range of physical, chemical, and mineralogical properties that evolve at varying rates. Soil scientists use various terms to describe these properties. A black, highly organic "A" horizon, for example, may form within a few centuries, while a dark brown, clayey "Bt" horizon may take as much as 40,000 years to form. Certain soil properties are invariably absent in young soils. For instance, soils developed in granitic alluvium of the San Joaquin Valley do not have Munsell hues redder than 10YR until they are at least 100,000 years old (Birkeland, 1999; Harden, 1982). Still other properties, such as the movement and deposition of clay-size particles and the precipitation of calcium carbonate at extraordinary depths, indicate soil formation during a climate much wetter than at present. In the absence of a radiometric age date for the material from which a particular soil formed, an estimate of its age must take into account all the known properties of the soil and the landscape and climate in which it evolved.

METHOD

The first step in studying a soil is the compilation of the data necessary for describing it (Birkeland, 1999; Borchardt, 2010). At minimum, this requires a Munsell

color chart, hand lens, acid bottle, meter for 1:1 soil:water pH and conductivity measurements. The second step may involve the collection of samples of each horizon for laboratory analysis of particle size. This is done to check the textural classifications made in the field and to evaluate the genetic relationships between horizons and between different soils in the landscape. When warranted, the clay mineralogy and chemistry of the soil also is analyzed to provide additional information on the changes undergone by the initial material from which the soil weathered. The last step is the comparison of this accumulated soil data with that for soils having developed under similar conditions. Such information is scattered in soil survey reports (e.g., Welch, 1981), soil science journals, and consulting reports. In a particular locality, there is seldom enough comparative data available for this purpose. That is why, at the very least, the study of one soil profile always makes the evaluation of the next that much easier.

RESULTS OF THIS EVALUATION

Soil Profile No. 1 was described in a Test Pit on a nearly level surface above a scarp of the Kings Canyon fault zone in a granitic alluvial fan (Figure 1 and Table 1). It was studied expressly to assess the age of the alluvial fan that was offset by the fault.

Soil Profile No. 1

This weakly developed profile was in a granitic alluvium mixture ranging from very fine sand to bouldery, saprolitic granite. The thin A horizon consisted of three parts: an 18-cm thick A overlying a 4-cm thick stoneline (2A) and an underlying 8-cm thick 3A (Figure 1). Horizons beneath the 3A consisted of a 48-cm thick 3B1tqm with a few thin patchy clay films bridging sand grains and a 46-cm thick 3B2tqm with very few clay films. The underlying 3CBq/Bt is a broken horizon consisting of two prominent parts: the 3CBq, which is relatively unoxidized, had a few granitic clasts with botryoidal silica precipitates on their bottoms (Figure 2). The Bt is a series of sub-horizontal clay lamellae (Figure 3) that have thin patchy clay films having yellowish brown colors (Figure 4). Soil pH decreased smoothly with depth from 6.9 in the surface to 5.6 at the base of the profile (Figure 5). Soil conductivity measurements show that the salt content of the A horizons is slightly elevated, perhaps because this is the locale of currently active soil weathering under this arid climate (Table 1; Figure 6).

DISCUSSION

Soil Profile No. 1 consists of three geological units. The A horizon is a very recent colluvial unit underlain by the 2A horizon, a stoneline that was deposited as the first phase of that colluviation. The underlying 3A horizon appears to be a remnant of the original A horizon that formed *in situ* along with the underlying soil horizons. The silica cementation at the 26-cm depth appears to mark the current wetting front, although the very recent erosion indicated by the stoneline makes this a minimum. It is true that precipitation also is now at 26 cm/yr, but loamy sand like this normally would produce a deeper wetting front. Clay loam, for instance, had weathering depths equivalent to mean annual precipitation

along the Hayward fault at Union City (Borchardt and Lienkaemper, 1994). The water holding capacity of loamy sand is much less than that of clay loam. The tiny amounts of clay observed in the 3Btqm horizons appear to have been translocated under a much wetter climate, as indicated by the clay lamellae seen at depths between 120 and 195-cm (Figure 1 and Figure 3). There has been much speculation about the formation of these clay lamellae (or "clay bands") (e.g., Dijkerman and others, 1967; Flach and others, 1974; Foss and Segovia, 1984; Gonzalez, 1993; Holliday and Rawling, 2006; Muhs, 1985; Schaetzl, 2001; Torrent and others, 1980; Warren, 1976).

They are invariably seen only in sandy soils. They have long been thought to have formed as temporary wetting fronts under a drying climate (e.g., Torrent and others, 1980). Clay in suspension stops moving when the precipitation becomes limiting (Figure 4). Once the clay at the wetting front settles out of suspension, it retards further movement in subsequent seasons having similar or greater precipitation. Then, as the climate becomes drier, the wetting front does not make it all the way to the previously formed lamellae—a new lamellae forms. Of course, aggradation of the surface can produce the same effect, which may explain the formation of those formed independently of a drying climate. Lamellae tend to form in sub-horizontal bands that become wavy when the texture of the parent material varies (Figure 3). Lamellae in this soil profile tend to be about 5 cm apart and about 4 mm thick. The ages of lamellae vary widely from 1 ka (Holliday and Rawling, 2006) to 122 ka (Torrent and others, 1980; Borchardt, 1993). A detailed study on the High Plains of Texas and New Mexico showed that the thickness (3 to 13 mm) and number (3 to 30) of the lamellae increased as a function of soil ages ranging from 1 to 14 ky B.P. (Holliday and Rawling, 2006).

It is likely that the silica cementation that followed Bt-horizon formation effectively prevented further clay translocation. It is possible that the silica source was from volcanic ash, perhaps from the Mazama and Tsoyawata (Bacon, 1983) eruptions from Crater Lake, Oregon at about 7 ka (Borchardt, 1969; Borchardt and Harward, 1971; Borchardt and others, 1971). Mazama is the most widespread Holocene volcanic ash in the western US. It has been found as far south as Mono Lake, where it was 14 cm above the Tsoyawata ash (Sarna-Wojcicki, and others, 1991). Nearest the site, it has been found at Honey Lake (Wills and Borchardt, 1993) and at Truckee, where it has been offset by faulting.

Volcanic glass dissolves readily in the acidic environment provided by granitic alluvium (Figure 5), with the siliceous solutions moving much farther than clay suspensions. That is probably why some botryoidal precipitates were seen on a few clasts in the 3CBq horizon (Figure 2).

CONCLUSIONS

1. This soil is about 15,000 years old.
2. This age is consistent with clay lamellae formation between the 120 and 195-cm depths, which is much too deep for modern precipitation, measured at only 26 cm, suggesting a drying climate provided by Pleistocene-Holocene transition.
3. The silica cementation seems to be a later, Holocene phenomenon.
4. I speculate that the ready source of silica may have involved the wind-blown addition of volcanic ash from Crater Lake at about 7 ka.

REFERENCES

Bacon, C.R., 1983, Eruptive history of Mount Mazama and Crater Lake caldera, Cascade Range, U.S.A: Journal of Volcanology and Geothermal Research, v. 18, p. 57-115.

Birkeland, P.W., 1999, Soils and geomorphology (3rd ed.): New York, Oxford University Press, 430 p.

Borchardt, Glenn,, 1970, Neutron activation analysis for correlating volcanic ash soils: Corvallis, Oregon State University, Ph.D. Thesis, 219 p.

Borchardt, Glenn, 1992, Pedochronology along the Hayward fault, *in* Borchardt, Glenn, Hirschfeld, S.E., Lienkaemper, J.J., McClellan, P., Williams, P.L., and Wong, I.G., eds., Proceedings of the Second Conference on Earthquake Hazards in the Eastern San Francisco Bay Area, California Department of Conservation, Division of Mines and Geology Special Publication 113, p. 111-117.

Borchardt, Glenn,, 1993, Pedochronological report for Harbor View Subdivision, Bodega Bay, California: Berkeley, CA, Soil Tectonics, 42 p.

Borchardt, Glenn, 1998, Soil tectonics: Geotimes, v. 36, p. 72-84.

Borchardt, Glenn, 2002, Mineralogy and soil tectonics, *in* Dixon, J. B., and Schulze, D. G., eds., Soil mineralogy with environmental applications: Soil Science Society of America Book Series No. 7: Madison, WI, Soil Science Society of America, p. 711-736.

Borchardt, Glenn, 2010, Soil stratigraphy for trench logging (3rd ed.): Berkeley, CA, Soil Tectonics, 67 p.

Borchardt, Glenn,, and Harward, M.E., 1971, Trace element correlation of volcanic ash soils: Soil Science Society of America Proceedings, v. 35, p. 626-631.

Borchardt, Glenn,, Harward, M.E., and Schmitt, R.A., 1971, Correlation of volcanic ash deposits by activation analysis of glass separates: Quaternary Research, v. 1, p. 247-260.

Borchardt, Glenn,, and Lienkaemper, J.J., 1994, Pedogenic calcite as an indicator of an early Holocene dry period in the San Francisco Bay Area [abs.], *in* Lanphere, M.A., Dalrymple, G.B., and Turrin, B.D., eds., Abstracts of the Eighth International Conference on Geochronology, Cosmochronology, and Isotope Geology: U.S. Geological Survey Circular 1107, p. 36.

Dijkerman, J.C., Cline, M.G., and Olson, G.W., 1967, Properties and genesis of textural subsoil lamellae: Soil Science, v. 104, p. 7-16.

Flach, K.W., Nettleton, W.D., and Nelson, R.E., 1974, The micromorphology of silica-cemented soil horizons in western North America, *in* Rutherford, G.K., ed., Soil microscopy: Kingston, Ontario, The Limestone Press, p. 714-729.

Foss, J.E., and Segovia, A.V., 1984, Rates of soil formation, *in* LaFleur, R.G., ed., Groundwater as a geomorphic agent: Boston, MA, Allen & Unwin Inc., p. 1-17.

Gonzalez, T., 1993, Use of soil lamellae as stratigraphic markers in fault investigations in the Los Angeles and Ventura basins [abs.], Association of Engineering Geologists Program and Abstracts 36th Annual Meeting, p. 50.

Harden, J.W., 1982, A quantitative index of soil development from field descriptions: Examples from a chronosequence in central California: Geoderma, v. 28, p. 1-23.

Holliday, V.T., and Rawling III, J.E., 2006, Soil-geomorphic relations of lamellae in eolian sand on the High Plains of Texas and New Mexico: Geoderma, v. 131, no. 1–2, p. 154-180.

Muhs, D.R., 1985, Age and paleoclimatic significance of Holocene sand dunes in northeastern Colorado: Annals of the Association of American Geographers, v. 75, no. 4, p. 566-582.

Sarna-Wojcicki, A.M., Lajoie, K.R., Meyer, C.E., Adam, D.P., and Rieck, H.J., 1991, Tephrochronologic correlation of upper Neogene sediments along the Pacific margin, conterminous United States, *in* Morrison, R.B., ed., Quaternary nonglacial geology: Conterminous U.S.: Boulder, CO, Geological Society of America The Geology of North America V. K-2, p. 117-140.

Schaetzl, R.J., 2001, Morphologic evidence of lamellae forming directly from thin, clayey bedding planes in a dune: Geoderma, v. 99, no. 1–2, p. 51-63.

Soil Survey Staff, 1992, Keys to soil taxonomy, 5th edition, SMSS Technical Monograph No. 19: Pocahontas Press, Inc., Blacksburg, VA, 541 p.

Soil Survey Staff, 1993, Soil survey manual (3rd edition): USDA-SCS Agriculture Handbook 18, U.S. Government Printing Office, Washington, DC, 457 p.

Soil Survey Staff, 1999, Soil taxonomy: A basic system of soil classification for making and interpreting soil surveys: USDA-SCS Agriculture Handbook 436, U.S. Government Printing Office, Washington, DC, 900 p.

Torrent, J., Nettleton, W.D., and Borst, G., 1980, Clay illuviation and lamella formation in a Psammentic Haploxeralf in southern California: Soil Science Society of America Journal, v. 44, p. 363-369.

Warren, A., 1976, Morphology and sediments of the Nebraska Sand Hills in relation to Pleistocene winds and the development of aeolian bedforms: Journal of Geology, v. 84, p. 685-700.

Wills, C.J., and Borchardt, Glenn,, 1993, Holocene slip rate and earthquake recurrence on the Honey Lake fault zone, northeastern California: Geology, v. 21, p. 853-856.

Welch, L. E., 1981, Soil survey of Alameda County, California, western part, U.S. Department of Agriculture, Soil Conservation Service in cooperation with University of California Agriculture Experiment Station, 103 p.

Table 1. Description of Soil Profile No. 1 from a Test Pit above Trench T-3 excavated across the Kings Canyon fault zone, Carson City, California. Abbreviations and definitions are given in Soil Survey Staff (1992; 1993; 1999).

Description of soil profile developed in alluvium by Glenn Borchardt, who measured and sampled the soil on August, 23, 2012 at about latitude N39.18° and longitude W119.80° in the south end wall of a Test Pit above Trench T-3. Desert climate with mean annual precipitation of 10.56"/yr (268 mm/yr) at Carson City from 1948-2005 (*Western Regional Climate Center, wrcc@dri.edu*). Sage. Slope 1%. Aspect south. Excellent drainage. Water deep. The parent material is sandy to bouldery Quaternary alluvium. Soil pH is neutral in the surface, becoming medium acid with depth. The soil is mapped as Surprise coarse sandy loam (*Aridic Haploxerolls)*.

Horizon	Depth, cm	Description
A	0-14	Very dark grayish brown (10YR3/2m, 5/2d) loamy sand with common fine distinct very pale brown (10YR8/3d) mottles due to feldspar grains; very fine weak granular structure; nonsticky and nonplastic when wet, very friable when moist, and soft when dry; common very fine roots; many very fine interstitial pores; abrupt smooth boundary; pH 6.9; conductivity 30 uS; Sample No. 12B411.
2A	14-18	Very dark grayish brown (10YR3/2m, 5/2d) cobbly loamy sand with common fine distinct very pale brown (10YR8/3d) mottles due to feldspar grains; very fine weak granular structure; nonsticky and nonplastic when wet, very friable when moist, and soft when dry; common very fine roots; many very fine interstitial pores; abrupt smooth boundary; stoneline sampled along with Sample No. 12B411 had flat lying cobbles, one of which was 7X3.5X3.5 cm.
3A	18-26	Very dark grayish brown (10YR3/2m, 5/2d) loamy sand with common fine distinct very pale brown (10YR8/3d) mottles due to feldspar grains; very fine moderate granular structure; nonsticky and nonplastic when wet, very friable when moist, and soft when dry; few very fine roots; many very fine interstitial pores; abrupt smooth boundary; pH 6.4; conductivity 20 uS; Sample No. 12B412.
3B1tqm	26-74	Olive brown (10YR4/3m, 6/3d) gravelly sand with many fine to medium prominent very pale brown (10YR8/3d) mottles due to feldspar grains; very fine moderate granular structure; nonsticky and nonplastic when wet, very friable when moist, and extremely hard when dry; many fine interstitial pores; few thin patchy clay films bridging sand grains; pH 6.0; conductivity 10 uS; Sample No. 12B413.
3B2tqm	74-120	Olive brown (10YR4/3m, 6/3d) gravelly sand and saprolitic cobble with many fine to medium prominent very pale brown (10YR8/3d) mottles due to feldspar grains; very fine moderate granular structure; nonsticky and nonplastic when wet, very friable when moist, and extremely hard when dry; many fine interstitial pores; very few thin patchy clay films bridging sand grains; diffuse smooth boundary; pH 5.8; conductivity 10 uS; Sample No. 12B414.

3CBq/Bt 120-195 Pale yellow (10YR7/4m, 8/4d) sandy gravel with many fine to medium prominent very pale brown (10YR8/3d) mottles due to feldspar grains; loose structure; nonsticky and nonplastic when wet, very friable when moist, and soft when dry; many fine interstitial pores; very few <1 mm thick silica deposits on granitic clasts; sub-horizontal 4-mm thick clay lamellae 5-10 cm apart with very few thin patchy clay films bridging sand grains (Bt); pH 5.6; conductivity 10 uS; Sample No. 12B415.

*ESTIMATED AGE:	t_o	=	15	ka
	t_b	=	0	ka
	t_d	=	15	ky

---

*Pedochronological estimates based on available information. All ages should be considered subject to ±50% variation unless otherwise indicated (Borchardt, 1992). Bold dates are absolute.

t_o = date when soil formation or aggradation began, ka

t_b = date when soil or strata was buried, ka

t_d = duration of soil development or aggradation, ky

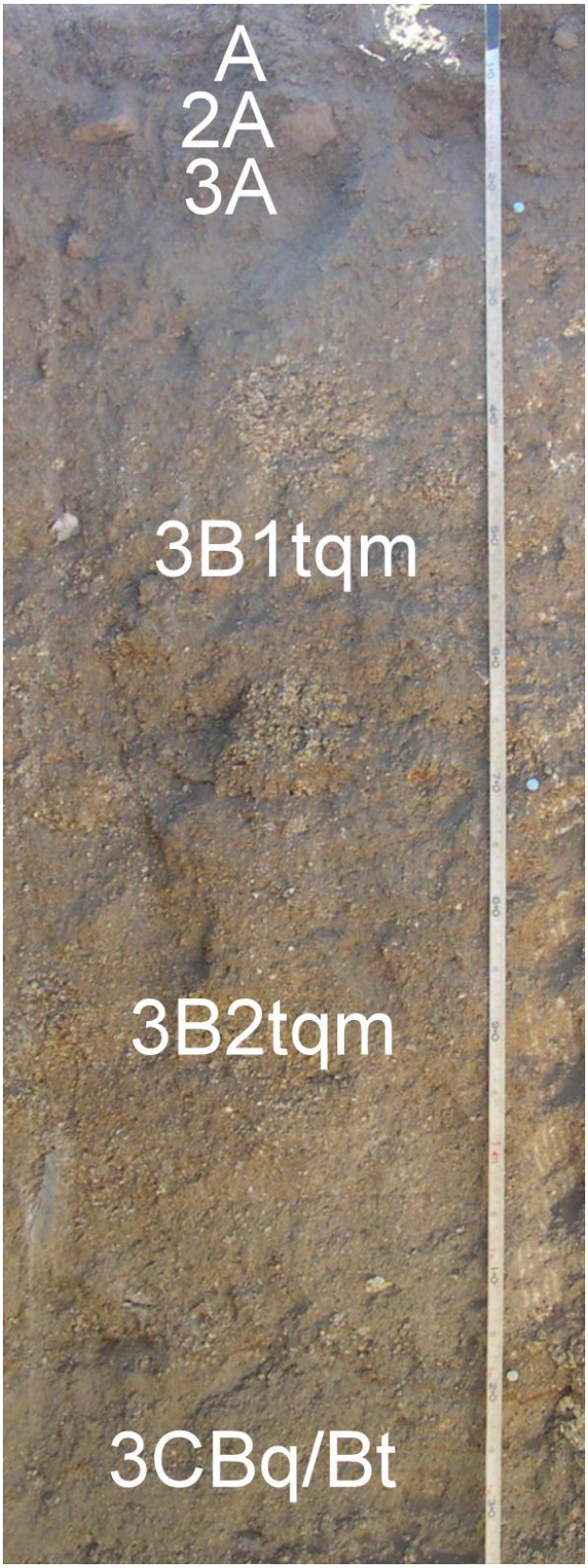

Figure 1. Soil Profile No. 1 on the alluvial fan above the Kings Canyon fault.

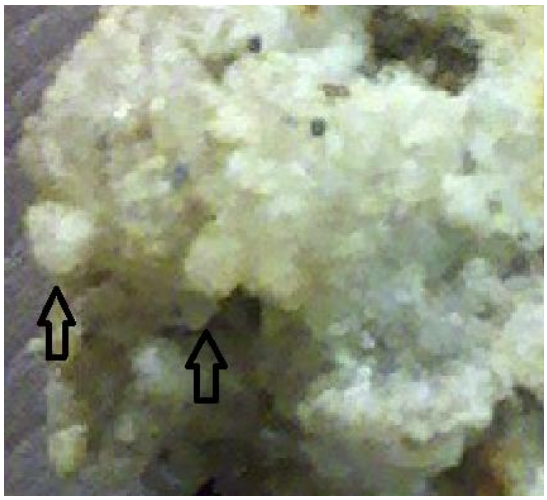

Figure 2. Spherical silica deposit (arrows) on bottom of granitic clast in the 3CBq horizon.

Figure 3. Clay lamellae (Bt) in the 3CBq/Bt horizon beneath the 120-cm depth.

Figure 4. Patchy clay films on clasts from one of the clay lamellae in the 3CBq/Bt horizon.

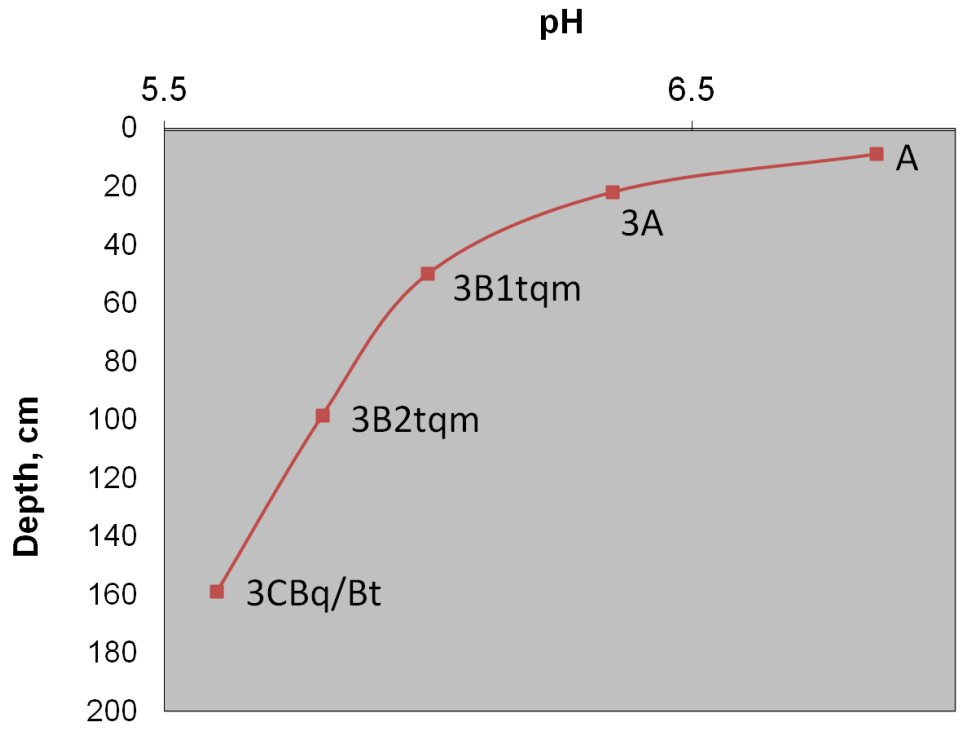

Figure 5. Soil pH showing the smooth decrease with depth.

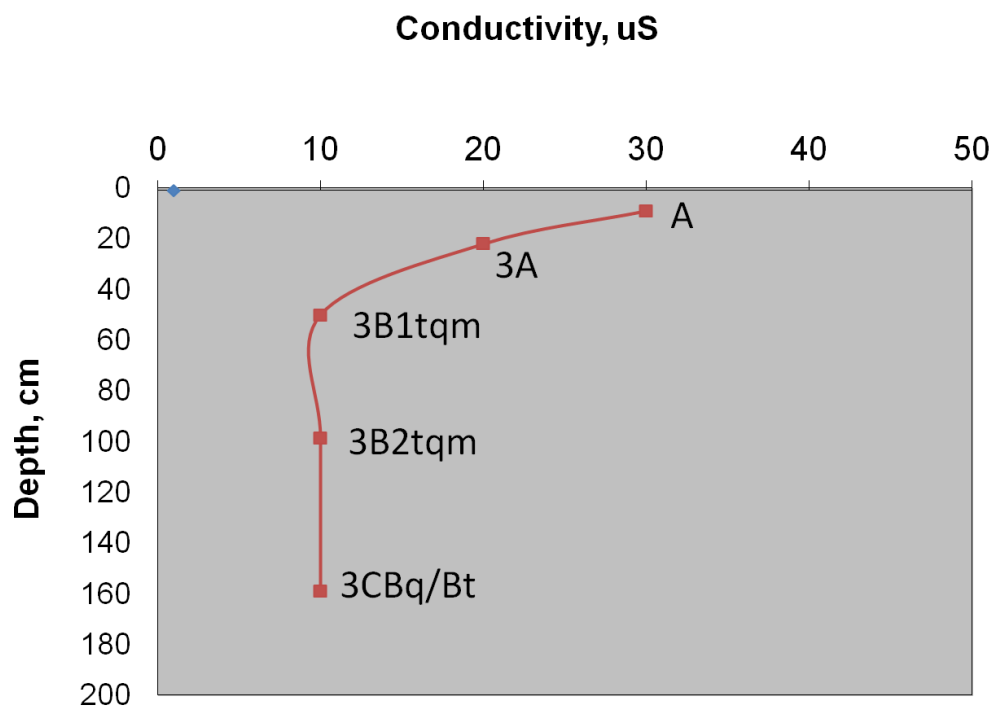

Figure 6. Depth function for conductivity showing that the surface horizons have more salt than the subsoil.

AGE. Elapsed time in calendar years. Because the cosmic production of C-14 has varied during the Quaternary, radiocarbon years (expressed as ky B.P.) must be corrected by using tree-ring and other data. Abbreviations used for corrected ages are: ka (kilo anno or years in thousands) or Ma (millions of years). Abbreviations used for intervals are: yr (years), ky (thousands of years). radiocarbon ages = yr B.P. Calibrated ages are calculated from process assumptions, relative ages fit in a sequence, and correlated ages refer to a matching unit. (See also yr B.P., HOLOCENE, PLEISTOCENE, QUATERNARY, PEDOCHRONOLOGY).
AGGRADATION. A modification of the earth's surface in the direction of uniformity of grade by deposition.
ALKALI (SODIC) SOIL. A soil having so high a degree of alkalinity (pH 8.5 or higher), or so high a percentage of exchangeable sodium (15 % or more of the total exchangeable bases), or both, that plant growth is restricted.
ALKALINE SOIL. Any soil that has a pH greater than 7.3. (See Reaction, Soil.)
ANGULAR ORPHANS. Angular fragments separated from weathered, well-rounded cobbles in colluvium derived from conglomerate.
ARGILLAN. (See Clay Film.)
ARGILLIC horizon. A horizon containing clay either translocated from above or formed in place through pedogenesis.
ALLUVIATION. The process of building up of sediments by a stream at places where stream velocity is decreased. The coarsest particles settle first and the finest particles settle last.
ANOXIC. (See also GLEYED SOIL). A soil having a low redox potential.
AQUICLUDE. A saturated body of sediment or rock that is incapable of transmitting significant quantities of water under ordinary hydraulic gradients.
AQUITARD. A body of rock or sediment that retards but does not prevent the flow of water to or from an adjacent aquifer. It does not readily yield water to wells or springs but may serve as a storage unit for groundwater.
ATTERBERG LIMITS. The moisture content at which a soil passes from a semi-solid to a plastic state (plastic limit, PL) and from a plastic to a liquid state (liquid limit, LL). The plasticity index (PI) is the numerical difference between the LL and the PL.
BEDROCK. The solid rock that underlies the soil and other unconsolidated material or that is exposed at the surface.
BISEQUUM. Two soils in vertical sequence, each soil containing an eluvial horizon and its underlying B horizon.
BOUDIN, BOUDINAGE. From a French word for sausage, describes the way that layers of rock break up under extension. Imagine the hand, fingers together, flat on the table, encased in soft clay and being squeezed from above, as being like a layer of rock. As the spreading clay moves the fingers (sausages) apart, the most mobile rock fractions are drawn or squeezed into the developing gaps.
BURIED SOIL. A developed soil that was once exposed but is now overlain by a more recently formed soil.
CALCAREOUS SOIL. A soil containing enough calcium carbonate (commonly with magnesium carbonate) to effervesce (fizz) visibly when treated with cold, dilute hydrochloric acid. A soil having measurable amounts of calcium carbonate or magnesium carbonate.
CARBONATE MORPHOLOGY STAGES. Descriptive classes of calcite precipitation indicating increasing pedogenesis over time:

	Stage	% $CaCO_3$
I	Bk horizon with few filaments and coatings	<10
I+	Bk with common filaments and continuous clast coatings	<10
II	Bk with continuous clast coatings, white masses, few nodules	>10
II+	Bk as above, but matrix is completely whitened, common nodules	>15
III	K horizon that is 90% white, many nodules	>20

III+	K that is completely plugged	>40
IV	K as above, but upper part cemented and has weak platy structure	>50
V	K same as above, but laminar layer is strong with incipient brecciation	>50
VI	K brecciation and recementation, as well as pisoliths, are common	>50

CATENA. A sequence of soils of about the same age, derived from similar parent material and forming under similar climatic conditions, but having different characteristics due to variation in relief and drainage. (See also TOPOSEQUENCE.)

CEC. Cation exchange capacity. The amount of negative charge balanced by positively charged ions (cations) that are exchangeable by other cations in solution (meq/100 g soil = cmol(+)/kg soil).

CLAY. As a soil separate, the mineral soil particles are less than 0.002 mm in diameter. As a soil textural class, soil material that is 40 percent or more clay, less than 45 percent sand, and less than 40 percent silt.

CLAY FILM. A coating of oriented clay on the surface of a sand grain, pebble, soil aggregate, or ped. Clay films also line pores or root channels and bridge sand grains. Frequency classification is based on the percent of the ped faces and/or pores that contain films: very few--<5%; few--5-25%; common--25-50%; many--50-90%; and continuous--90-100%. Thickness classification is based on visibility of sand grains: thin--very fine sand grains standout; moderately thick--very fine sand grains impart microrelief to film; thick--fine sand grains enveloped by clay and films visible without magnification. Synonyms: clay skin, clay coat, argillan, illuviation cutan.

CLAY LAMELLAE. Thin, generally wavy bands that appear as multiple micro-Bt horizons at the base of the solum in sandy Holocene deposits. The lamellae generally are 1-3 cm in thickness and 5 to 30 cm apart. There may be two to six or more clay lamellae comprising the Bt horizon of such a soil.

COBBLE. Rounded or partially rounded fragments of rock ranging from 7.5 to 25 cm in diameter.

COLLUVIUM. Any loose mass of soil or rock fragments that moves downslope largely by the force of gravity. Usually it is thicker at the base of the slope.

COLLUVIUM-FILLED SWALE. The prefailure topography of the source area of a debris flow.

COMPARATIVE PEDOLOGY. The comparison of soils, particularly through examination of features known to evolve through time.

CONCRETIONS. Grains, pellets, or nodules of various sizes, shapes, and colors consisting of concentrated compounds or cemented soil grains. The composition of most concretions is unlike that of the surrounding soil. Calcium carbonate and iron oxide are common compounds in concretions.

CONDUCTIVITY. The ability of a soil solution to conduct electricity, generally expressed as the reciprocal of the electrical resistivity. Electrical conductance is the reciprocal of the resistance (1/R = 1/ohm = ohm^{-1} = mho [reverse of ohm] = siemens = S), while electrical conductivity is the reciprocal of the electrical resistivity (EC = 1/r = 1/ohm-cm = mho/cm = S/cm or mmho/cm = dS/m). EC, expressed as uS/cm, is equivalent to the ppm of salt in solution when multiplied by 0.640. Pure rain water has an EC of 0, standard 0.01 N KCl is 1411.8 uS at 25C, and the growth of salt-sensitive crops is restricted in soils having saturation extracts with an EC greater than 2,000 uS/cm. Measurements in soils are usually performed on 1:1 suspensions containing one part by weight of soil and one part by weight of distilled water.

CONSISTENCE, SOIL. The feel of the soil and the ease with which a lump can be crushed by the fingers. Terms commonly used to describe consistence are --

Loose.--Noncoherent when dry or moist; does not hold together in a mass.

Friable.--When moist, crushes easily under gentle pressure between thumb and forefinger and can be pressed together into a lump.

Firm.--When moist, crushes under moderate pressure between thumb and forefinger, but resistance is distinctly noticeable.

Plastic.--When wet, readily deformed by moderate pressure but can be pressed into a lump; will

form a "wire" when rolled between thumb and forefinger.
Sticky.--When wet, adheres to other material, and tends to stretch somewhat and pull apart, rather than to pull free from other material.
Hard.--When dry, moderately resistant to pressure; can be broken with difficulty between thumb and forefinger.
Soft.--When dry, breaks into powder or individual grains under very slight pressure.
Cemented.--Hard and brittle; little affected by moistening.
CTPOT. Easily remembered acronym for climate, topography, parent material, organisms, and time; the five factors of soil formation.
CUMULIC. A soil horizon that has undergone aggradation coincident with its active development.
CUTAN. (See Clay Film.)
DEBRIS FLOW. Incoherent or broken masses of rock, soil, and other debris that move downslope in a manner similar to a viscous fluid.
DEBRIS SLOPE. A constant slope with debris on it from the free face above.
DEGRADATION. A modification of the earth's surface by erosion.
DURIPAN. A subsurface soil horizon that is cemented by illuvial silica, generally deposited as opal or microcrystalline silica, to the degree that less than 50 percent of the volume of air-dry fragments will slake in water or HCl.
ELUVIATION. The removal of soluble material and solid particles, mostly clay and humus, from a soil horizon by percolating water.
EOLIAN. Deposits laid down by the wind, landforms eroded by the wind, or structures such as ripple marks made by the wind.
FAULT-LINE SCARP. A scarp that has been produced by differential erosion along an old fault line.
FAULTSLIDE. A landslide that shows physical evidence of its interaction with a fault.
FIRST-ORDER DRAINAGE. The most upstream, field-discernible concavity that conducts water and sediments to lower parts of a watershed.
FLOOD PLAIN. A nearly level alluvial plain that borders a stream and is subject to flooding unless protected artificially.
FOSSIL FISSURE. A buried rectilinear chamber associated with extension due to ground movement. The chamber must be oriented along the strike of the shear and must have vertical and horizontal dimensions greater than its width. It must show no evidence of faunal activity and its walls may have silt or clay coatings indicative of frequent temporary saturation with ground water. May be mistaken for an animal burrow. Also known as a paleofissure.
FRIABILITY. Term for the ease with which soil crumbles. A friable soil is one that crumbles easily.
GENESIS, SOIL. The mode of origin of the soil. Refers especially to the processes or soil-forming factors responsible for the formation of the solum (A and B horizons) from the unconsolidated parent material.
GEOMORPHIC. Pertaining to the form of the surface features of the earth. Specifically, geomorphology is the analysis of landforms and their mode of origin.
GLEYED SOIL. A soil having one or more neutral gray horizons as a result of water logging and lack of oxygen. The term "gleyed" also designates gray horizons and horizons having yellow and gray mottles as a result of intermittent water logging.
GRAVEL. Rounded or angular fragments of rock 2 to 75 mm in diameter. Soil textures with >15% gravel have the prefix "gravelly" and those with >90% gravel have the suffix "gravel."
HIGHSTAND. The highest elevation reached by the ocean during an interglacial period.
HOLOCENE. The most recent epoch of geologic time, extending from 10 ka to the present.
HORIZON, SOIL. A layer of soil, approximately parallel to the surface, that has distinct characteristics produced by soil-forming processes. These are the major soil horizons:
O horizon.--The layer of organic matter on the surface of a mineral soil. This layer consists of decaying plant residues.
A horizon.--The mineral horizon at the surface or just below an O horizon. This horizon is the one

in which living organisms are most active and therefore is marked by the accumulation of humus. The horizon may have lost one or more of soluble salts, clay, and sesquioxides (iron and aluminum oxides).

E horizon -- This eluvial horizon is light in color, lying beneath the A horizon and above the B horizon. It is made up mostly of sand and silt, having lost most of its clay and iron oxides through reduction, chelation, and translocation.

B horizon.--The mineral horizon below an A horizon. The B horizon is in part a layer of change from the overlying A to the underlying C horizon. The B horizon also has distinctive characteristics caused (1) by accumulation of clay, sesquioxides, humus, or some combination of these; (2) by prismatic or blocky structure; (3) by redder or stronger colors than the A horizon; or (4) by some combination of these.

C horizon.--The relatively unweathered material immediately beneath the solum. Included are sediment, saprolite, organic matter, and bedrock excavatable with a spade. In most soils this material is presumed to be like that from which the overlying horizons were formed. If the material is known to be different from that in the solum, a number precedes the letter C.

R horizon.--Consolidated rock not excavatable with a spade. It may contain a few cracks filled with roots or clay or oxides. The rock usually underlies a C horizon but may be immediately beneath an A or B horizon.

Major horizons may be further distinguished by applying prefix Arabic numbers to designate differences in parent materials as they are encountered (e.g., 2B, 2BC, 3C) or by applying suffix numerals to designate minor changes (e.g., B1, B2).

The following is from Soil Survey Staff (2006):

“Suffix Symbols

Lowercase letters are used as suffixes to designate specific kinds of master horizons and layers. The term “accumulation” is used in many of the definitions of such horizons to indicate that these horizons must contain more of the material in question than is presumed to have been present in the parent material. The suffix symbols and their meanings are as follows:

a Highly decomposed organic material

This symbol is used with O to indicate the most highly decomposed organic materials, which have a fiber content of less than 17 percent (by volume) after rubbing.

b Buried genetic horizon

This symbol is used in mineral soils to indicate identifiable buried horizons with major genetic features that were developed before burial. Genetic horizons may or may not have formed in the overlying material, which may be either like or unlike the assumed parent material of the buried soil. This symbol is not used in organic soils, nor is it used to separate an organic layer from a mineral layer.

c *Concretions or nodules*

This symbol indicates a significant accumulation of concretions or nodules. Cementation is required. The cementing agent commonly is iron, aluminum, manganese, or titanium. It cannot be silica, dolomite, calcite, or more soluble salts.

co *Coprogenous earth*

This symbol, used only with L, indicates a limnic layer of coprogenous earth (or sedimentary peat).

d *Physical root restriction*

This symbol indicates noncemented, root-restricting layers in natural or human-made sediments or materials. Examples are dense basal till, plowpans, and other mechanically compacted zones.

di *Diatomaceous earth*

This symbol, used only with L, indicates a limnic layer of diatomaceous earth.

e *Organic material of intermediate decomposition*

This symbol is used with O to indicate organic materials of intermediate decomposition. The fiber content of these materials is 17 to 40 percent (by volume) after rubbing.

f *Frozen soil or water*

This symbol indicates that a horizon or layer contains permanent ice. The symbol is not used for seasonally frozen layers or for dry permafrost.

ff *Dry permafrost*

This symbol indicates a horizon or layer that is continually colder than 0 oC and does not contain enough ice to be cemented by ice. This suffix is not used for horizons or layers that have a temperature warmer than 0 oC at some time of the year.

g *Strong gleying*

This symbol indicates either that iron has been reduced and removed during soil formation or that saturation with stagnant water has preserved it in a reduced state. Most of the affected layers have chroma of 2 or less, and many have redox concentrations. The low chroma can represent either the color of reduced iron or the color of uncoated sand and silt particles from which iron has been removed. The symbol g is not used for materials of low chroma that have no history of wetness, such as some slates or E horizons. If g is used with B, pedogenic change in addition to gleying is implied. If no other pedogenic change besides gleying has taken place, the horizon is designated Cg.

h *Illuvial accumulation of organic matter*

This symbol is used with B to indicate the accumulation of illuvial, amorphous, dispersible complexes of organic matter and sesquioxides if the sesquioxide component is dominated by aluminum but is present only in very small quantities. The organo-sesquioxide material coats sand and silt particles. In some horizons these coatings have coalesced, filled pores, and cemented the horizon. The symbol h is also used in combination with s as “Bhs” if the amount of the sesquioxide component is significant but the color value and chroma, moist, of the horizon are 3 or less.

i *Slightly decomposed organic material*

This symbol is used with O to indicate the least decomposed of the organic materials. The fiber content of these materials is 40 percent or more (by volume) after rubbing.

j *Accumulation of jarosite*

Jarosite is a potassium or iron sulfate mineral that is commonly an alteration product of pyrite that has been exposed to an oxidizing environment. Jarosite has hue of 2.5Y or yellower and normally has chroma of 6 or more, although chromas as low as 3 or 4 have been reported. [Note: No longer used to indicate “juvenile.”]

jj *Evidence of cryoturbation*

Evidence of cryoturbation includes irregular and broken horizon boundaries, sorted rock fragments, and organic soil materials existing as bodies and broken layers within and/or between mineral soil layers. The organic bodies and layers are most commonly at the contact between the active layer and the permafrost.

k *Accumulation of secondary carbonates*

This symbol indicates an accumulation of visible pedogenic calcium carbonate (less than 50 percent, by volume). Carbonate accumulations exist as carbonate filaments, coatings, masses, nodules, disseminated carbonate, or other forms.

kk *Engulfment of horizon by secondary carbonates*

This symbol indicates major accumulations of pedogenic calcium carbonate. The suffix kk is used when the soil fabric is plugged with fine grained pedogenic carbonate (50 percent or more, by volume) that exists as an essentially continuous medium. The suffix corresponds to the stage III plugged horizon or higher of the carbonate morphogenetic stages (Gile et al., 1966).

m *Cementation or induration*

This symbol indicates continuous or nearly continuous cementation. It is used only for horizons that are more than 90 percent cemented, although they may be fractured. The cemented layer is physically root-restrictive. The dominant cementing agent (or the two dominant ones) may be indicated by adding defined letter suffixes, singly or in pairs. The horizon suffix km indicates cementation by carbonates; qm, cementation by silica; sm, cementation by iron; ym, cementation by gypsum; kqm, cementation by lime and silica; and zm, cementation by salts more soluble than

gypsum.
ma *Marl*
This symbol, used only with L, indicates a limnic layer of marl.
n *Accumulation of sodium*
This symbol indicates an accumulation of exchangeable sodium.
o *Residual accumulation of sesquioxides*
This symbol indicates a residual accumulation of sesquioxides.
p *Tillage or other disturbance*
This symbol indicates a disturbance of the surface layer by mechanical means, pasturing, or similar uses. A disturbed organic horizon is designated Op. A disturbed mineral horizon is designated Ap even though it is clearly a former E, B, or C horizon.
q *Accumulation of silica*
This symbol indicates an accumulation of secondary silica.
r *Weathered or soft bedrock*
This symbol is used with C to indicate cemented layers (moderately cemented or less cemented). Examples are weathered igneous rock and partly consolidated sandstone, siltstone, or slate. The excavation difficulty is low to high.
s *Illuvial accumulation of sesquioxides and organic matter*
This symbol is used with B to indicate an accumulation of illuvial, amorphous, dispersible complexes of organic matter and sesquioxides if both the organic-matter and sesquioxide components are significant and if either the color value or chroma, moist, of the horizon is 4 or more. The symbol is also used in combination with h as “Bhs” if both the organic-matter and sesquioxide components are significant and if the color value and chroma, moist, are 3 or less.
ss *Presence of slickensides*
This symbol indicates the presence of slickensides. Slickensides result directly from the swelling of clay minerals and shear failure, commonly at angles of 20 to 60 degrees above horizontal. They are indicators that other vertic characteristics, such as wedge-shaped peds and surface cracks, may be present.
t *Accumulation of silicate clay*
This symbol indicates an accumulation of silicate clay that either has formed *in situ* within a horizon or has been moved into the horizon by illuviation, or both. At least some part of the horizon should show evidence of clay accumulation either as coatings on surfaces of peds or in pores, as lamellae, or as bridges between mineral grains.
u *Presence of human-manufactured materials (artifacts)*
This symbol indicates the presence of manufactured artifacts that have been created or modified by humans, usually for a practical purpose in habitation, manufacturing, excavation, or construction activities. Examples of artifacts are processed wood products, liquid petroleum products, coal, combustion by-products, asphalt, fibers and fabrics, bricks, cinder blocks, concrete, plastic, glass, rubber, paper, cardboard, iron and steel, altered metals and minerals, sanitary and medical waste, garbage, and landfill waste.
v *Plinthite*
This symbol indicates the presence of iron-rich, humus-poor, reddish material that is firm or very firm when moist and hardens irreversibly when exposed to the atmosphere and to repeated wetting and drying.
w *Development of color or structure*
This symbol is used with B to indicate the development of color or structure, or both, with little or no apparent illuvial accumulation of material. It should not be used to indicate a transitional horizon.
x *Fragipan character*
This symbol indicates a genetically developed layer that has a combination of firmness and brittleness and commonly a higher bulk density than the adjacent layers. Some part of the layer is

physically root-restrictive.
y *Accumulation of gypsum*
This symbol indicates an accumulation of gypsum.
z *Accumulation of salts more soluble than gypsum*
This symbol indicates an accumulation of salts that are more soluble than gypsum."
HUMUS. The well-decomposed, more or less stable part of the organic matter in mineral soils.
ILLUVIATION. The deposition by percolating water of solid particles, mostly clay or humus, within a soil horizon.
INTERFLUVE. The land lying between streams.
ISOCHRONOUS BOUNDARY. A gradational boundary between two sedimentary units indicating that they are approximately the same age. Opposed to a nonisochronous boundary, which by its abruptness indicates that it delineates units having significant age differences.
KROTOVINA. An animal burrow filled with soil.
LEACHING. The removal of soluble material from soil or other material by percolating water.
LOWSTAND. The lowest elevation reached by the ocean during a glacial period.
MANGAN. A thin coating of manganese oxide (cutan) on the surface of a sand grain, pebble, soil aggregate, or ped. Mangans also line pores or root channels and bridge sand grains.
MODERN SOIL. The portion of a soil section that is under the influence of current pedogenetic conditions. It generally refers to the uppermost soil regardless of age.
MODERN SOLUM. The combination of the A and B horizons in the modern soil.
MORPHOLOGY, SOIL. The physical make-up of the soil, including the texture, structure, porosity, consistence, color, and other physical, mineral, and biological properties of the various horizons, and the thickness and arrangement of those horizons in the soil profile.
MOTTLING, SOIL. Irregularly marked with spots of different colors that vary in number and size. Mottling in soils usually indicates poor aeration and lack of drainage. Descriptive terms are as follows: abundance--few, common, and many; size--fine, medium, and coarse; and contrast--faint, distinct and prominent. The size measurements are these: fine, less than 5 mm in diameter along the greatest dimension; medium, from 5 to 15 mm, and coarse, more than 15 mm.
MRT (MEAN RESIDENCE TIME.) The average age of the carbon atoms within a soil horizon. Under ideal reducing conditions, the humus in a soil will have a C-14 age that is half the true age of the soil. In oxic soils humus is typically destroyed as fast as it is produced, generally yielding MRT ages no older than 300-1000 years, regardless of the true age of the soil.
MUNSELL COLOR NOTATION. Scientific description of color determined by comparing soil to a Munsell Soil Color Chart (Available from Macbeth Division of Kollmorgen Corp., 2441 N. Calvert St., Baltimore, MD 21218). For example, dark yellowish brown is denoted as 10YR3/4m in which the 10YR refers to the hue or proportions of yellow and red, 3 refers to value or lightness (0 is black and 10 is white), 4 refers to chroma (0 is pure black and white and 20 is the pure color), and m refers to the moist condition rather than the dry (d) condition.
OVERBANK DEPOSIT. Fine-grained alluvial sediments deposited from floodwaters outside of the fluvial channel.
OXIC. A soil having a high redox potential. Such soils typically are well drained, seldom being waterlogged or lacking in oxygen. Rubification in such soils tends to increase with age.
PALEO SOIL TONGUE. A soil tongue that formed during a previous soil-forming interval.
PALEOSEISMOLOGY. The study of prehistoric earthquakes through the examination of soils, sediments, and rocks.
PALEOSOL. A soil that formed on a landscape in the past with distinctive morphological features resulting from a soil-forming environment that no longer exists at the site. The former pedogenic process was either altered because of external environmental change or interrupted by burial.
PALINSPASTIC RECONSTRUCTION. Diagrammatic reconstruction used to obtain a picture of what geologic and/or soil units looked like before their tectonic deformation.
PARENT MATERIAL. The great variety of unconsolidated organic and mineral material in which soil

forms. Consolidated bedrock is not yet parent material by this concept.
PED. An individual natural soil aggregate, such as a granule, a prism, or a block.
PEDOCHRONOLOGY. The study of pedogenesis with regard to the determination of when soil formation began, how long it occurred, and when it stopped. Also known as soil dating. Two ages and the calculated duration are important:
t_o = age when soil formation or aggradation began, ka
t_b = age when the soil or stratum was buried, ka
t_d = duration of soil development or aggradation, ky
Pedochronological estimates are based on available information. All ages should be considered subject to $\pm$50% variation unless otherwise indicated.
PEDOCHRONOPALEOSEISMOLOGY. The study of prehistoric earthquakes by using pedochronology.
PEDOLOGY. The study of the process through which rocks, sediments, and their constituent minerals are transformed into soils and their constituent minerals at or near the surface of the earth.
PEDOGENESIS. The process through which rocks, sediments, and their constituent minerals are transformed into soils and their constituent minerals at or near the surface of the earth.
PERCOLATION. The downward movement of water through the soil.
pH VALUE. The negative log of the hydrogen ion concentration. Measurements in soils are usually performed on 1:1 suspensions containing one part by weight of soil and one part by weight of distilled water. A soil with a pH of 7.0 is precisely neutral in reaction because it is neither acid nor alkaline. An acid or "sour" soil is one that gives an acid reaction; an alkaline soil is one that gives an alkaline reaction. In words, the degrees of acidity or alkalinity are expressed as:

Extremely acid------- <4.5
Very strongly acid--- 4.5 to 5.0
Strongly acid-------- 5.1 to 5.5
Medium acid---------- 5.6 to 6.0
Slightly acid-------- 6.1 to 6.5
Neutral---------- 6.6 to 7.3
Mildly alkaline------ 7.4 to 7.8
Moderately alkaline-- 7.9 to 8.4
Strongly alkaline---- 8.5 to 9.0
Very strongly alkaline >9.0
Used if significant:
Very slightly acid--- 6.6 to 6.9
Very mildly alkaline- 7.1 to 7.3

PHREATIC SURFACE. (See Water Table.)
PLANATION. The process of erosion whereby a portion of the surface of the Earth is reduced to a fundamentally even, flat, or level surface by a meandering stream, waves, currents, glaciers, or wind.
PLEISTOCENE. An epoch of geologic time extending from 10 ka to 1.8 Ma; it includes the last Ice Age.
PROFILE, SOIL. A vertical section of the soil through all its horizons and extending into the parent material.
QUATERNARY. A period of geologic time that includes the past 1.8 Ma. It consists of two epochs--the Pleistocene and Holocene.
PROGRADATION. The building outward toward the sea of a shoreline or coastline by nearshore deposition.
RELICT SOIL. A surface soil that was partly formed under climatic conditions significantly different from the present.
RUBIFICATION. The reddening of soils through the release and precipitation of iron as an oxide

during weathering. Munsell hues and chromas of well-drained soils generally increase with soil age.
SALINE SOIL. A soil that contains soluble salts in amounts that impair the growth of crop plants but that does not contain excess exchangeable sodium.
SAND. Individual rock or mineral fragments in a soil that range in diameter from 0.05 to 2.0 mm. Most sand grains consist of quartz, but they may be of any mineral composition. The textural class name of any soil that contains 85 percent or more sand and not more than 10 percent clay.
SECONDARY FAULT. A minor fault that bifurcates from or is associated with a primary fault. Movement on a secondary fault never occurs independently of movement on the primary, seismogenic fault.
SHORELINE ANGLE. The line formed by the intersection of the wave-cut platform and the sea cliff. It approximates the position of sea level at the time the platform was formed.
SILT. Individual mineral particles in a soil that range in diameter from the upper limit of clay (0.002 mm) to the lower limit of very find sand (0.05 mm.) Soil of the silt textural class is 80 percent or more silt and less than 12 percent clay.
SLICKENSIDES. Polished and grooved surfaces produced by one mass sliding past another. In soils, slickensides may form along a fault plane; at the bases of slip surfaces on steep slopes; on faces of blocks, prisms, and columns undergoing shrink-swell. In tectonic slickensides the striations are strictly parallel.
SLIP RATE. The rate at which the geologic materials on the two sides of a fault move past each other over geologic time. The slip rate is expressed in mm/yr, and the applicable duration is stated. Faults having slip rates less than 0.01 mm/yr are generally considered inactive, while faults with Holocene slip rates greater than 0.1 mm/yr generally display tectonic geomorphology.
SMECTITE. A fine, platy, aluminosilicate clay mineral that expands and contracts with the absorption and loss of water. It has a high cation-exchange capacity and is plastic and sticky when moist.
SOIL. A natural, three-dimensional body at the earth's surface that is capable of supporting plants and has properties resulting from the integrated effect of climate and living matter acting on earthy parent material, as conditioned by relief over periods of time.
SOIL SEISMOLOGIST. Soil scientist who studies the effects of earthquakes on soils.
SOIL SLICKS. Curvilinear striations that form in swelling clayey soils, where there is marked change in moisture content. Clayey slopes buttressed by rigid materials may allow minor amounts of gravitationally driven plastic flow, forming soil slicks sometimes mistaken for evidence of tectonism. Soil slicks disappear with depth and the striations are seldom strictly parallel as they are when movement is major. (See also SLICKENSIDES.)
SOIL TECTONICS. The study of the interactions between soil formation and tectonism.
SOIL TONGUE. That portion of a soil horizon extending into a lower horizon.
SOLUM. Combined A and B horizons. Also called the true soil. If a soil lacks a B horizon, the A horizon alone is the solum.
STONELINE. A thin, buried, planar layer of stones, cobbles, or bedrock fragments. Stonelines of geological origin may have been deposited upon a former land surface. The fragments are more often pebbles or cobbles than stones. A stoneline generally overlies material that was subject to weathering, soil formation, and erosion before deposition of the overlying material. Many stonelines seem to be buried erosion pavements, originally formed by running water on the land surface and concurrently covered by surficial sediment.
STRATH TERRACE. A gently sloping terrace surface bearing little evidence of aggradation.
STRUCTURE, SOIL. The arrangement of primary soil particles into compound particles or aggregates that are separated from adjoining aggregates. The principal forms of soil structure are--platy (laminated), prismatic (vertical axis of aggregates longer than horizontal), columnar (prisms with rounded tops), blocky (angular or subangular), and granular. Structureless soils are either single grained (each grain by itself, as in dune sand) or massive (the particles adhering without any

regular cleavage, as in many hardpans).
SUBSIDIARY FAULT. A branch fault that extends a substantial distance from the main fault zone.
TECTOTURBATION. Soil disturbance resulting from tectonic movement.
TEXTURE, SOIL. Particle size classification of a soil, generally given in terms of the USDA system which uses the term "loam" for a soil having equal properties of sand, silt, and clay. The basic textural classes, in order of their increasing proportions of fine particles are sand, loamy sand, sandy loam, loam, silt loam, silt, sandy clay loam, clay loam, silty clay loam, sand clay, silty clay, and clay. The sand, loamy sand, and sandy loam classes may be further divided by specifying "coarse," "fine," or "very fine."
TOPOSEQUENCE. A sequence of kinds of soil in relation to position on a slope. (See also CATENA.)
TRANSLOCATION. The physical movement of soil particles, particularly fine clay, from one soil horizon to another under the influence of gravity.
UNIFIED SOIL CLASSIFICATION SYSTEM. The particle size classification system used by the U.S. Army Corps of Engineers and the Bureau of Reclamation. Like the ASTM and AASHO systems, the sand/silt boundary is at 80 um instead of 50 um used by the USDA. Unlike all other systems, the gravel/sand boundary is at 4 mm instead of 2 mm and the silt/clay boundary is determined by using Atterberg limits.
VERTISOL. A soil with at least 30% clay, usually smectite, that fosters pronounced changes in volume with change in moisture. Cracks greater than 1 cm wide appear at a depth of 50 cm during the dry season each year. One of the ten USDA soil orders.
WATER TABLE. The upper limit of the soil or underlying rock material that is wholly saturated with water. Also called the phreatic surface.
WAVE-CUT PLATFORM. The relatively smooth, slightly seaward-dipping surface formed along the coast by the action of waves generally accompanied by abrasive materials.
WEATHERING. All physical and chemical changes produced in rocks or other deposits at or near the earth's surface by atmospheric agents. These changes result in disintegration and decomposition of the material.
WETTING FRONT. The greatest depth affected by moisture due to precipitation.
yr B.P. Uncorrected radiocarbon age expressed in years before present, calculated from 1950. Calendar-corrected ages are expressed in ka, or, if warranted, as A.D. or B.C.

Appendix B

EXAMINATION OF BULK SOIL FROM
THE KINGS CANYON FAULT 2012 TRENCHING SITE,
CARSON CITY, NEVADA

By

Kathryn Puseman,
Peter Kováčik, and
Linda Scott Cummings

With assistance from
R.A. Varney

PaleoResearch Institute
Golden, Colorado

PaleoResearch Institute Technical Report 13-046

Prepared for

University of Nevada, Nevada Bureau of Mines and Geology
Reno, Nevada

September 2013

INTRODUCTION

Seven bulk soil samples from the Kings Canyon Fault 2012 Trenching Site were collected from two trenches excavated on an alluvial fan in a weak mollic environment supporting a high desert sagebrush-bunchgrass community. “Deposits likely range from latest Pleistocene to late Holocene and are from tectonic colluvial wedges buttressed against a fault” (Craig dePolo, personal communication, April 2013). These samples were examined for the presence of charred organic material suitable for AMS radiocarbon determination. In the absence of larger-sized charred remains, two of the samples were extracted to recover microscopic charcoal for dating. Two AMS radiocarbon dates were obtained for microscopic charcoal extracted from these samples.

METHODS Flotation and

Identification

The bulk samples were floated using a modification of the procedures outlined by Matthews (1979). Each sample was added to approximately 3 gallons of water. The sample was stirred until a strong vortex formed, which was allowed to slow before pouring the light fraction through a 150-micron-mesh sieve. All material that passed through the screen was retained for possible microcharcoal, particulate soil organics, and/or humate extraction. Additional water was added and the process repeated until all visible macrofloral material was removed from the sample (a minimum of five times). The material that remained in the bottom (the heavy fraction) was poured through a 0.5-mm-mesh screen. The floated portions were allowed to dry.

The light fractions were weighed, then passed through a series of graduated screens (US Standard Sieves with 4-mm, 2-mm, 1-mm, 0.5-mm, and 0.25-mm openings) to separate the charcoal debris and to initially sort the remains. The contents of each screen then were examined. Charcoal fragments were broken to expose fresh cross, radial, and tangential sections, then examined under a binocular microscope at a magnification of 70x and under a Nikon Optiphot 66 microscope at magnifications of 320–800x. The remaining light fraction in the 4-mm, 2-mm, 1-mm, 0.5-mm, and 0.25-mm sieves was scanned under a binocular stereo microscope at a magnification of 10x, with some identifications requiring magnifications of up to 70x. The material that passed through the 0.25-mm screen was not examined. The coarse or heavy fractions also were screened and examined for the presence of botanic remains. Remains from both the light and heavy fractions were recorded as charred and/or uncharred, whole and/or fragments. The term "seed" is used to represent seeds, achenes, caryopses, and other disseminules.

The macrofloral remains, including charcoal, were identified using manuals (Carlquist 2001; Hoadley 1990; Martin and Barkley 1961; Musil 1963)
(Panshin and de Zeeuw 1980; Schopmeyer 1974) and by comparison with modern and archaeological references. Because charcoal and possibly other botanic remains were to be submitted for radiocarbon dating, clean laboratory conditions were used during flotation and identification to avoid contamination. All instruments were washed between samples, and the samples were protected from contact with modern charcoal.

Microcharcoal Recovery and AMS Radiocarbon Dating

It is now possible to recover microscopic charcoal and particulate soil organics from sediments for the purpose of obtaining an AMS radiocarbon age. A chemical extraction technique based on that used for pollen, and relying upon heavy liquid extraction, has been modified to recover microscopic charcoal and particulate soil organics for the purpose of obtaining an AMS radiocarbon age. Hydrochloric (HCl) acid (10%) was added to the material retained from flotation that had passed through the 250 micron mesh sieve to remove calcium carbonates. The samples then were rinsed until neutral, and a small quantity of sodium hexametaphosphate was added to begin clay removal. Sample beakers then were filled with reverse osmosis deionized (RODI) water and allowed to settle according to Stoke's Law. After two hours, the supernatant, containing clay, was poured off and the sample was rinsed with RODI water three more times, being allowed to settle according to Stoke's Law to remove more clays. Once the clays had been removed, the samples were freeze-dried. Sodium polytungstate (SPT) with a density of 1.8 was used for the flotation process. The samples were mixed with SPT and centrifuged at 1500 rpm for 10 minutes to separate organic from inorganic remains. The supernatant containing pollen, organic remains, and microscopic charcoal was decanted. Sodium polytungstate again was added to the inorganic fraction to repeat the separation process until all visible material had been recovered. The microscopic charcoal fragments were recovered from the sodium polytungstate by diluting this mixture with RODI and centrifuging, after which they were rinsed thoroughly with RODI water. Following this step, the samples were examined using a binocular microscope at a magnification of up to 30x to check the matrix for charcoal and particulate soil organics. This mixture of charcoal and particulate soil organics was then subjected to a nitric acid treatment in which a small quantity of concentrated nitric acid was added to each sample tube, which was then placed in hot sand to cover the level of nitric acid for a period of approximately 10-20 minutes, depending on need. Following this treatment the samples were rinsed copiously with RODI water, then examined again using a binocular microscope at a magnification of up to 30x to check for the presence of charcoal and particulate organics. When all of the particulate organics have been removed the sample receives a few drops of dilute HCl to return it to a slightly acid state. Microscopic charcoal fragments were then sealed in a microcentrifuge tube.

Standards and laboratory background wood samples were simultaneously treated to the same acid and base processing as the microscopic charcoal samples of unknown age, with the exception that they were not subjected to the concentrated, hot nitric acid bath because it oxidizes unburned material. A radiocarbon "dead" wood blank from the Grey Fossil site in Washington County, Tennessee, that is believed to date to the Hemphillian stage of the late Miocene, 4.5-7 MYA (currently beyond the detection capabilities of AMS) was used to calibrate the laboratory correction factor. Standards of known age, such as TIRI Sample "B" (Belfast Pine) with a consensus age of 4503 ± 6, and TIRI Sample "J" (Bulston Crannog wood) with a consensus age of 1605 ± 8 (Gulliksen and Scott 1995), also were used to establish the laboratory correction factor. Each wood standard was run in a quantity similar to the submitted samples of unknown age and sealed in a quartz tube after the requisite pre-treatment.

Once all the wood standards, blanks, and submitted microcharcoal samples of unknown age were prepared and sealed in their individual quartz tubes, they were combusted at 820 °C, soaked for an extended period of time at that temperature, and then slowly allowed to cool to enable the chemical reaction that extracts carbon dioxide (CO_2) gas.

Following this last step, microcharcoal samples of unknown age, the wood standards, and the laboratory backgrounds were sent to the Center for Applied Isotope Studies in Athens, Georgia, where the CO_2 gas was processed into graphite. The graphite in these samples then was placed in the target and run through the accelerator, which produces the numbers that are converted into the radiocarbon date presented in the data section. Dates are presented as conventional radiocarbon ages, as well as calibrated ages using Intcalc04 curves on Oxcal version 3.10 (Bronk Ramsey 2005; Reimer et al. 2009). This is a probability-based method for determining conventional ages and is preferred over the intercept-based alternative because it provides a calibrated date that reflects the probability of its occurrence within a given distribution (reflected by the amplitude (height) of the curve), as opposed to individual point estimates. As a result, the probability-based method offers more stability to the calibrated values than those derived from intercept-based methods that are subject to adjustments in the calibration curve (Telford et al. 2004).

RADIOCARBON REVIEW

When interpreting radiocarbon dates from non-annuals such as trees and shrubs, it is important to understand that a radiocarbon date reflects the age of that portion of the tree/shrub when it stopped exchanging carbon with the atmosphere, not necessarily the date that the tree/shrub died or was burned. Trees and shrubs grow bigger each year from the cambium, where a new layer or ring of cells is added each year. During photosynthesis, new cells take in atmospheric carbon dioxide, which includes radiocarbon. The radiocarbon taken in will reflect the radiocarbon present in the atmosphere during that season of growth. Once the sapwood in a tree has been converted into heartwood, the metabolic process stops for that inner wood. Once this happens, no new carbon atoms are acquired, and the radiocarbon that is present starts to decay. Studies have shown that there is little to no movement of carbon-bearing material from one ring to another. As a result, wood from different parts of the tree will yield different radiocarbon dates. The outer rings exhibit an age close to the cutting or death date of the tree, while the inner rings will reflect the age of the tree. Because the younger, outer rings burn off first when a log or branch is burned, it is the older, inner rings that typically are what is left remaining in a charcoal assemblage (Puseman 2009; Taylor 1987).

DISCUSSION

Seven bulk soil samples were collected from two trenches excavated on an alluvial fan at the Kings Canyon Fault 2012 Trenching Site, Nevada (Table 1). These samples were examined for presence of charred organic material suitable for AMS radiocarbon determination.

Sample KC2-R1 yielded three fragments of charred parenchymous tissue weighing 0.0022 g (Table 2 and 3). Parenchyma is the botanical term for relatively undifferentiated tissue composed of many similar cells with thin primary walls. Parenchyma occurs in many different plant tissues in varying amounts, especially large fleshy organs such as roots and stems, but also in fruits, seeds, cones, periderm (bark), leaves, needles, etc. (Hather 2000:1; Mauseth 1988). Charcoal from this sample consist of twelve pieces of unidentified hardwood (0.0023 g) reflecting broad-leaved flowering tree or shrub, that was too small and too vitrified for further

identification. This sample yielded sufficient charcoal for radiocarbon dating, although vitrified charcoal usually looses a significant mass during chemical pre-treatment. A single piece of uncharred *Festuca* floret, rootlets, muscovite, rocks and pieces of rodent fecal pellet were also noted in the sample.

A total of 42 fragments of unidentified hardwood charcoal, weighing 0.0118 g were recovered from Sample KC3-R2. These charcoal fragments are sufficient for radiocarbon dating. Three fragments of charred parenchymous tissue (0.0009 g) were present in this sample. No other charred remains were recovered. A single fragment of uncharred seed, few leaf fragments, few periderm fragments, and moderate rootlets represent modern plants growing in the project area.

Sample KC3-R3 contained three fragments of charred parenchymous tissue (0.0008 g), four fragments of charred organic material (0.0022 g) and a moderate amount of rootlets. Nine pieces of unidentified hardwood charcoal weighing 0.0024 g provides sufficient charcoal for AMS radiocarbon dating. It is also possible to combine this charcoal with other charred material identified in this sample.

Three fragments of charred parenchymous tissue weighing 0.0008 g, and twenty-one pieces of unidentified hardwood charcoal weighing 0.0012 g were present in Sample KC3-R4 providing a sufficient amount of charred remains for AMS radiocarbon analysis.

Sample KC3-R5 consists of few uncharred fragments of periderm and few rootlets. This sample also yielded eighteen fragments of unidentified hardwood charcoal weighing 0.0007 g. A sample of this size is small for radiocarbon dating as the mass will most likely be lost during chemical pre-treatment; however, a successful date is still possible.

Few fragments of uncharred periderm, few rootlets, and three fragments of unidentified hardwood charcoal (0.0001 g) were recovered from Sample KC3-R7, while eight pieces of unidentifiable charcoal weighing less than 0.0001 g were recovered in Sample KC3-R6. Samples KC3-R7 and KC3-R6 yielded few very small fragments of charcoal, in addition to rootlets, muscovite, and rock. Although these macroscopic charcoal fragments were not sufficient for dating, they indicated that the sediment had the potential to yield microscopic charcoal that could be extracted to obtain a radiocarbon date. Recovery of microcharcoal from Sample KC3-R6 yielded 0.0015 g, while Sample KC3-R6 returned 0.0020 g of mass. These samples were submitted for AMS radiocarbon dating. Microscopic charcoal has a significantly different surface to volume ratio than most macroscopic charcoal, resulting in loss of a portion of this mass during chemical pre-treatment. The microcharcoal in Sample KC3-R7 returned a date of 405 ± 24 RCYBP (PRI-13-046-KC3-R7), with a two-sigma calibrated age range of 520-430 and 360-330 CAL yr. BP or AD 1430-1520 and AD 1590-1620 (Table 4, Figures 1 and 2). A date of 329 ± 22 RCYBP (PRI-13-046-KC3-R6) was returned for microcharcoal in Sample KC3-R6, which calibrates to an age range of 470-300 CAL yr. BP or AD 1480-1650 (Figure 3 and 4) at the two-sigma level. While there is overlap in these calibrations, it is primarily the result of the date for KC3-R7 being located just prior to and intersecting with a flat spot in the calibration curve (Figure 5). Sample KC3-R6 intersects primarily with the same flat spot on the calibration curve, then extends beyond to the next downward trend in the curve. The calibration curve for the Late Holocene exhibits several intervals of relatively flat to slightly increasing quantities of carbon, resulting in calibrations with long calendar year ranges.

SUMMARY AND CONCLUSIONS

Macrofloral analysis of bulks soil samples from the Kings Canyon Fault 2012 Trenching Site, Nevada yielded few charred organic remains, such as parenchymous tissue and small pieces of charcoal. Samples KC2-R1, KC3-R2, KC3-R3, KC3-R4, and KC3-R5 yielded sufficient amounts of charcoal or other charred organic remains for possible AMS radiocarbon determination. Very small pieces of charcoal were present in Samples KC3-R7 and KC3-R6, in quantities not sufficient for dating. Microscopic charcoal extracted from these two samples yielded dates of 405 ± 24 RCYBP and 329 ± 22 RCYBP, which overlap significantly at the two-sigma level. These dates indicate these sediments date to the Late Holocene.

TABLE 1
PROVENIENCE DATA FOR SAMPLES FROM
THE KINGS CANYON FAULT 2012 TRENCHING SITE, NEVADA

Trench No.	Sample No.	Sample Description/ Provenience	Analysis
2	KC2-R1	Bulk soil sample from stacked colluvial deposits burying and derived from an adjacent fault scarp, part of the silica cemented unit speculated to be the result of a weathering ash fall on the surface	Float/Charcoal ID
3	KC3-R2	Bulk soil sample from stacked colluvial deposits burying and derived from an adjacent fault scarp	Float/Charcoal ID
	KC3-R3	Bulk soil sample from stacked colluvial deposits burying and derived from an adjacent fault scarp	Float/Charcoal ID
	KC3-R4	Bulk soil sample from stacked colluvial deposits burying and derived from an adjacent fault scarp	Float/Charcoal ID
	KC3-R5	Bulk soil sample from stacked colluvial deposits burying and derived from an adjacent fault scarp	Float/Charcoal ID
	KC3-R7	Bulk soil sample from stacked colluvial deposits burying and derived from an adjacent fault scarp, part of the silica cemented unit speculated to be the result of a weathering ash fall on the surface	Microcharcoal AMS ^{14}C Date
	KC3-R6	Bulk soil sample from a massive buttressed colluvial deposit, derived from fluvial sands	Microcharcoal AMS ^{14}C Date

TABLE 2
MACROFLORAL REMAINS FROM THE KINGS CANYON FAULT 2012 TRENCHING SITE, NEVADA

Sample No.	Identification	Part	Charred W	Charred F	Uncharred W	Uncharred F	Weights/ Comments
KC2-R1	Liters Floated						1.80 L
	Light Fraction Weight						2.567 g
	FLORAL REMAINS:						
	Parenchymous tissue - vitrified			3			0.0022 g
	Festuca	Floret			1		
	Rootlets					X	Moderate
	CHARCOAL/WOOD:						
	Unidentified hardwood - small, vitrified	Charcoal		12			0.0023 g
	NON-FLORAL REMAINS:						
	Muscovite					X	Moderate
	Rock					X	Numerous
	Rodent fecal pellet - small				X	X	Few
KC3-R2	Liters Floated						2.00 L
	Light Fraction Weight						2.532 g
	FLORAL REMAINS:						
	Parenchymous tissue			3			0.0009 g
	Erodium	Seed				1	
	Leaf					X	Few
	Periderm					X	Few
	Rootlets					X	Moderate
	CHARCOAL/WOOD:						
	Unidentified hardwood - small	Charcoal		42			0.0118 g
	NON-FLORAL REMAINS:						
	Muscovite					X	Few
	Rock					X	Numerous
	Rodent fecal pellet - small				X	X	Moderate
KC3-R3	Liters Floated						2.00 L
	Light Fraction Weight						1.880 g
	FLORAL REMAINS:						
	Parenchymous tissue			3			0.0008 g
	Unidentified organic material			4			0.0022 g
	Rootlets					X	Moderate

TABLE 2 (Continued)

Sample No.	Identification	Part	Charred W	Charred F	Uncharred W	Uncharred F	Weights/ Comments
KC3-R3	CHARCOAL/WOOD:						
	Unidentified hardwood - small	Charcoal		9			0.0024 g
	NON-FLORAL REMAINS:						
	Muscovite					X	Numerous
	Rock					X	Numerous
KC3-R4	Liters Floated						1.80 L
	Light Fraction Weight						1.097 g
	FLORAL REMAINS:						
	Parenchymous tissue			3			0.0008 g
	Periderm					X	Few
	Rootlets					X	Moderate
	CHARCOAL/WOOD:						
	Unidentified hardwood - small	Charcoal		21			0.0012 g
	NON-FLORAL REMAINS:						
	Muscovite					X	Moderate
	Rock					X	Numerous
KC3-R5	Liters Floated						2.20 L
	Light Fraction Weight						0.803 g
	FLORAL REMAINS:						
	Periderm					X	Few
	Rootlets					X	Few
	CHARCOAL/WOOD:						
	Unidentified hardwood - small	Charcoal		18			0.0007 g
	NON-FLORAL REMAINS:						
	Insect (Ant head)	Chitin				1	
	Muscovite					X	Numerous
	Rock					X	Numerous
KC3-R7	Liters Floated						1.50 L
	Light Fraction Weight						0.582 g
	FLORAL REMAINS:						
	Periderm					X	Few
	Rootlets					X	Few

TABLE 2 (Continued)

Sample No.	Identification	Part	Charred W	Charred F	Uncharred W	Uncharred F	Weights/ Comments
KC3-R7	CHARCOAL/WOOD:						
	Unidentified hardwood - small	Charcoal		3			0.0001 g
	NON-FLORAL REMAINS:						
	Insect	Chitin				1	
	Muscovite					X	Numerous
	Rock					X	Numerous
KC3-R6	Liters Floated						1.70 L
	Light Fraction Weight						0.321 g
	FLORAL REMAINS:						
	Rootlets					X	Few
	CHARCOAL/WOOD:						
	Unidentifiable - small	Charcoal		8			<0.0001 g
	NON-FLORAL REMAINS:						
	Muscovite					X	Numerous
	Rock					X	Numerous

W = Whole
F = Fragment
X = Presence noted in sample
L = Liters
g = grams

TABLE 3
INDEX OF MACROFLORAL REMAINS RECOVERED FROM THE
KINGS CANYON FAULT 2012 TRENCHING SITE, NEVADA

Scientific Name	Common Name
FLORAL REMAINS:	
Erodium	Storksbill, Filaree
Festuca	Fescue
Parenchymous tissue	Relatively undifferentiated tissue composed of many similar cells with thin primary walls–occurs in different plant organs in varying amounts, especially large fleshy organs such as roots and stems, but also fruits, seeds, cones, periderm (bark), leaves, needles, etc.
Periderm	Technical term for bark; Consists of the cork (phellum) which is produced by the cork cambium, as well as any epidermis, cortex, and primary or secondary phloem exterior to the cork cambium
CHARCOAL/WOOD:	
Unidentified hardwood - small	Wood from a broad-leaved flowering tree or shrub, fragments too small for further identification
Unidentified hardwood - vitrified	Wood from a broad-leaved flowering tree or shrub, exhibiting a shiny, glassy appearance due to fusion by heat
NON-FLORAL REMAINS:	
Chitin	A natural polymer found in insect and crustacean exoskeleton
Muscovite	The most common mica, found in granites, pegmatites, gneisses and schists, with a layered structure of aluminum silicate sheets weakly bonded together by layers of potassium ions

TABLE 4
RADIOCARBON RESULTS FOR SAMPLES FROM
THE KINGS CANYON FAULT 2012 TRENCHING SITE, NEVADA

Sample No.	Sample Identification	AMS ^{14}C Date*	1-sigma Calibrated Date (68.2%)	2-sigma Calibrated Date (95.4%)	$*^{13}C$** ($^{o}/_{oo}$)
PRI-13-046-KC3-R7	Microcharcoal	405 ± 24 RCYBP	510-465 CAL yr. BP	520-430; 360-330 CAL yr. BP	-26.14
			AD 1440-1485	AD 1430-1520 AD 1590-1620	
PRI-13-046-KC3-R6	Microcharcoal	329 ± 22 RCYBP	440-310 CAL yr. BP	470-300 CAL yr. BP	-24.7
			AD 1510-1640	AD 1480-1650	

* Reported in radiocarbon years at 1 standard deviation measurement precision (68.2%), corrected for $*^{13}C$.

** $*^{13}C$ values are measured by AMS during the ^{14}C measurement . The AMS-$*^{13}C$ values are used for the ^{14}C calculation and should not be used for dietary or paleoenvironmental interpretations.

PaleoResearch Institute
2675 Youngfield Street, Golden, CO 80401
(303) 277-9848 • Fax (303) 462-2700
www.paleoresearch.com

FIGURE 1. PRI RADIOCARBON AGE CALIBRATION

Laboratory Number: PRI-13-046-KC3-R7
Sample Identification: Microcharcoal
Conventional AMS ^{14}C Date: 405 ± 24 RCYBP
1-sigma Calibrated Age Range (68.2%): 510-465 CAL yr. BP
2-sigma Calibrated Age Range (95.4%): 520-430; 360-330 CAL yr. BP
$*^{13}C$ ($^{o}/_{oo}$): -26.14 (Measured for ^{14}C calculation, not valid for dietary or paleoenvironmental interpretations)

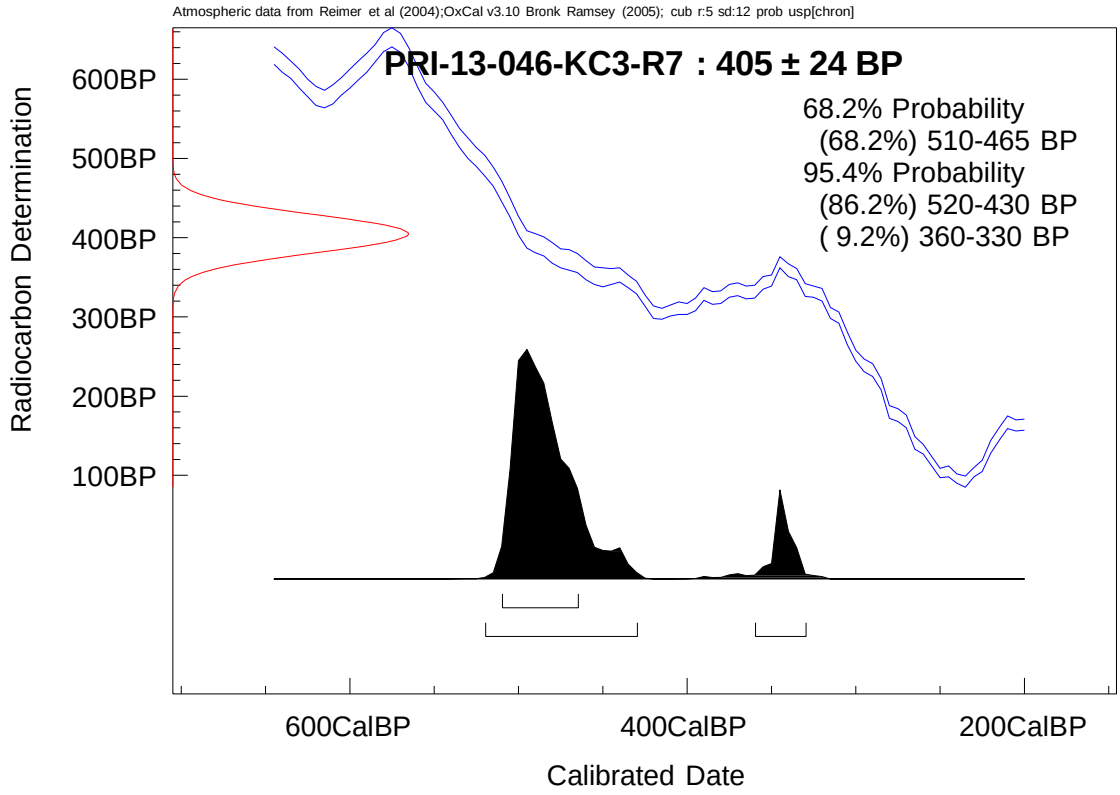

Intercept Statement. For radiocarbon calibration, PRI uses OxCal3.10 (Bronk Ramsey 2005), which is a probability-based method for converting ages in radiocarbon years (RCYBP) into calibrated dates (CAL yr BP). This method is preferred over the intercept-based alternative because instead of providing individual point estimates, it reflects the probability of the date's occurrence within a given range (reflected by the amplitude [height] of the curve). As a result, the probability-based method produces more stable calibrated values than do intercept-based methods (Telford 2004). Ongoing refinements and adjustments to the calibration curve have a greater apparent effect on individual points than on ranges.

References

Bronk Ramsey, C., 2005, OxCal. 3.1 ed. www.rlaha.ox.ac.uk/oxcal/oxcal.htm.

Reimer, P. J., M. G. L. Baillie, E. Bard, A. Bayliss, J. W. Beck, P.G. Blackwell, C. Bronk Ramsey, C. E. Buck, G. S. Burr, R. L. Edwards, M. Friedrich, P. M. Grootes, T. P. Guilderson, I. Hajdas, T. J. Heaton, A. G. Hogg, K. A. Hughen, K. F. Kaiser, B. Kromer, F. G. McCormac, S. W. Manning, R. W. Reimer, D. A. Richards, J. R. Southon, S. Talamo, C. S. M. Turney, J. van der Plicht, C. E. Weyhenmeyer. 2009. IntCal09 and Marine09 radiocarbon age calibration curves, 0-50,000 years cal BP. *Radiocarbon* 51(4):1111–1150.

Telford, R. J., E. Heegaard, and H. J. B. Birks, 2004, *The Holocene* 14(2):296-298.

PaleoResearch Institute
2675 Youngfield Street, Golden, CO 80401
(303) 277-9848 • Fax (303) 462-2700
www.paleoresearch.com

FIGURE 2. PRI RADIOCARBON AGE CALIBRATION

Laboratory Number: PRI-13-046-KC3-R7
Sample Identification: Microcharcoal
Conventional AMS ^{14}C Date: 405 ± 24 RCYBP
1-sigma Calibrated Age Range (68.2%): AD 1440-1485
2-sigma Calibrated Age Range (95.4%): AD 1430-1520; AD 1590-1620
$*^{13}C$ ($^{o}/_{oo}$): -26.14 (Measured for ^{14}C calculation, not valid for dietary or paleoenvironmental interpretations)

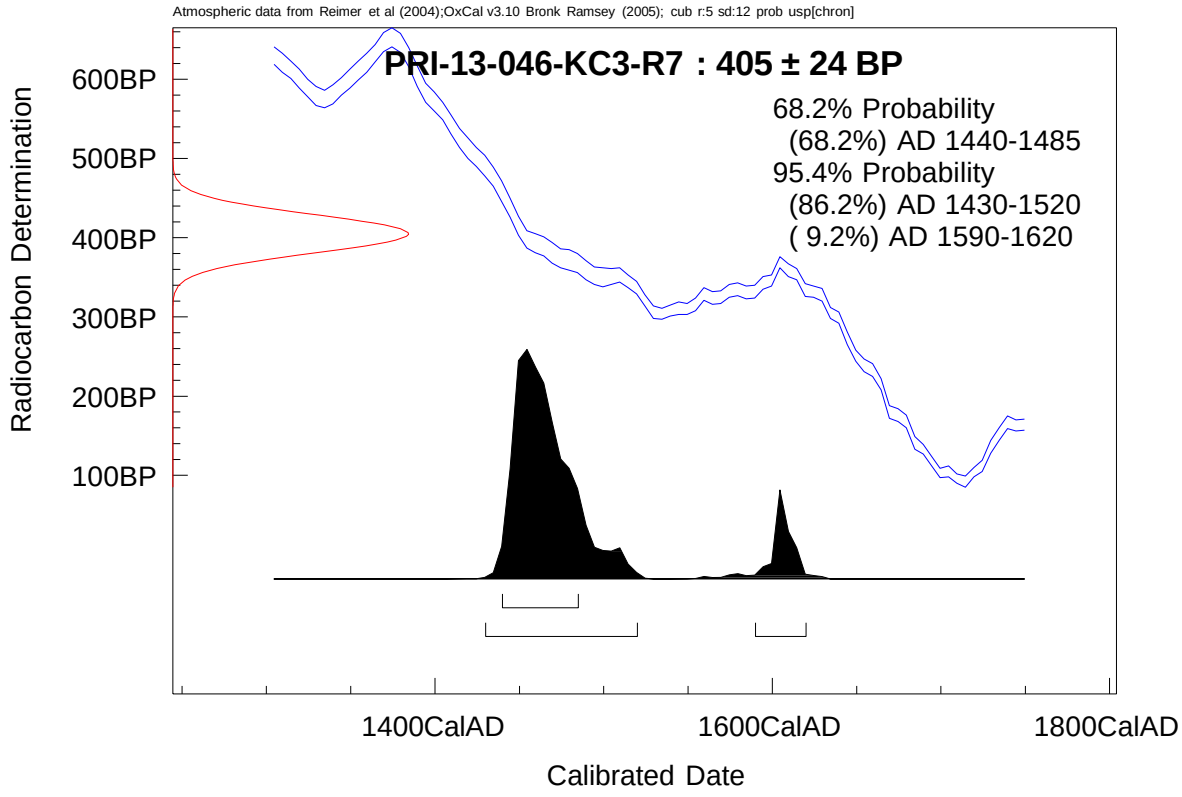

Intercept Statement. For radiocarbon calibration, PRI uses OxCal3.10 (Bronk Ramsey 2005), which is a probability-based method for converting ages in radiocarbon years (RCYBP) into calibrated dates (CAL yr BP). This method is preferred over the intercept-based alternative because instead of providing individual point estimates, it reflects the probability of the date's occurrence within a given range (reflected by the amplitude [height] of the curve). As a result, the probability-based method produces more stable calibrated values than do intercept-based methods (Telford 2004). Ongoing refinements and adjustments to the calibration curve have a greater apparent effect on individual points than on ranges.

References

Bronk Ramsey, C., 2005, OxCal. 3.1 ed. www.rlaha.ox.ac.uk/oxcal/oxcal.htm.

Reimer, P. J., M. G. L. Baillie, E. Bard, A. Bayliss, J. W. Beck, P.G. Blackwell, C. Bronk Ramsey, C. E. Buck, G. S. Burr, R. L. Edwards, M. Friedrich, P. M. Grootes, T. P. Guilderson, I. Hajdas, T. J. Heaton, A. G. Hogg, K. A. Hughen, K. F. Kaiser, B. Kromer, F. G. McCormac, S. W. Manning, R. W. Reimer, D. A. Richards, J. R. Southon, S. Talamo, C. S. M. Turney, J. van der Plicht, C. E. Weyhenmeyer. 2009. IntCal09 and Marine09 radiocarbon age calibration curves, 0-50,000 years cal BP. *Radiocarbon* 51(4):1111–1150.

Telford, R. J., E. Heegaard, and H. J. B. Birks, 2004, *The Holocene* 14(2):296-298.

PaleoResearch Institute
2675 Youngfield Street, Golden, CO 80401
(303) 277-9848 • Fax (303) 462-2700
www.paleoresearch.com

FIGURE 3. PRI RADIOCARBON AGE CALIBRATION

Laboratory Number: PRI-13-046-KC3-R6
Sample Identification: Microcharcoal
Conventional AMS ^{14}C Date: 329 ± 22 RCYBP
1-sigma Calibrated Age Range (68.2%): 440-310 CAL yr. BP
2-sigma Calibrated Age Range (95.4%): 470-300 CAL yr. BP
$*^{13}C$ ($^{o}/_{oo}$): -24.7 (Measured for ^{14}C calculation, not valid for dietary or paleoenvironmental interpretations)

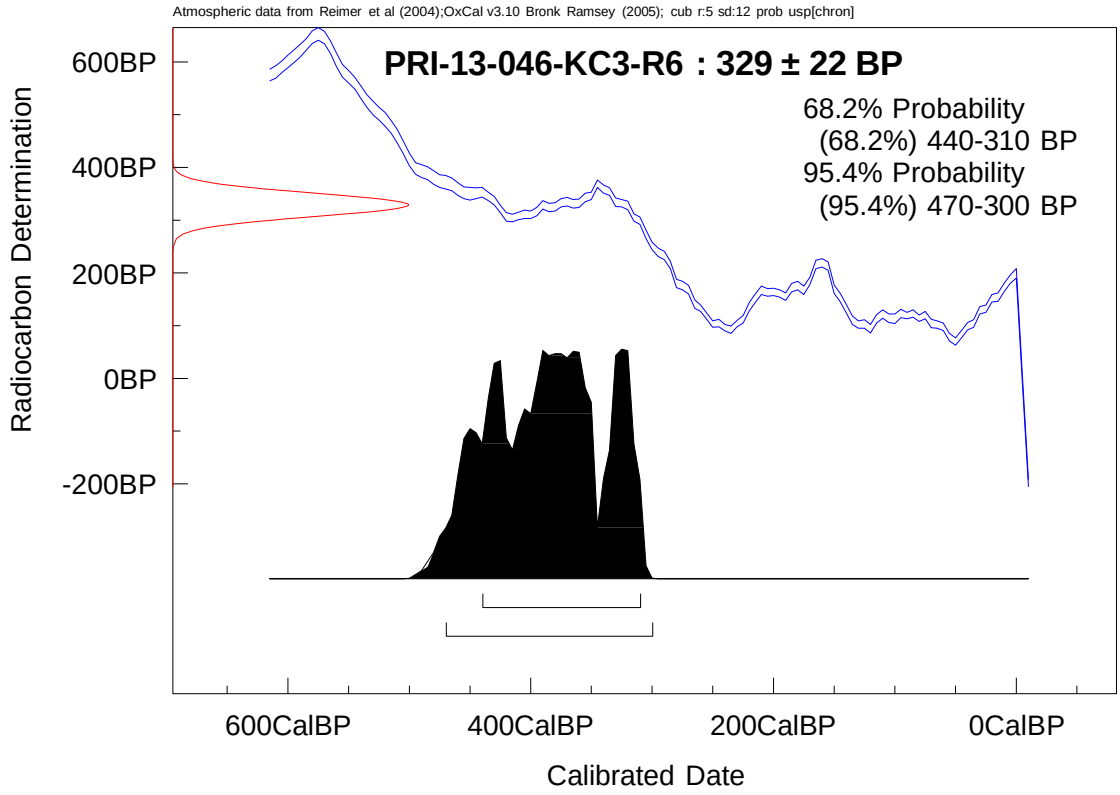

Intercept Statement. For radiocarbon calibration, PRI uses OxCal3.10 (Bronk Ramsey 2005), which is a probability-based method for converting ages in radiocarbon years (RCYBP) into calibrated dates (CAL yr BP). This method is preferred over the intercept-based alternative because instead of providing individual point estimates, it reflects the probability of the date's occurrence within a given range (reflected by the amplitude [height] of the curve). As a result, the probability-based method produces more stable calibrated values than do intercept-based methods (Telford 2004). Ongoing refinements and adjustments to the calibration curve have a greater apparent effect on individual points than on ranges.

References

Bronk Ramsey, C., 2005, OxCal. 3.1 ed. www.rlaha.ox.ac.uk/oxcal/oxcal.htm.

Reimer, P. J., M. G. L. Baillie, E. Bard, A. Bayliss, J. W. Beck, P.G. Blackwell, C. Bronk Ramsey, C. E. Buck, G. S. Burr, R. L. Edwards, M. Friedrich, P. M. Grootes, T. P. Guilderson, I. Hajdas, T. J. Heaton, A. G. Hogg, K. A. Hughen, K. F. Kaiser, B. Kromer, F. G. McCormac, S. W. Manning, R. W. Reimer, D. A. Richards, J. R. Southon, S. Talamo, C. S. M. Turney, J. van der Plicht, C. E. Weyhenmeyer. 2009. IntCal09 and Marine09 radiocarbon age calibration curves, 0-50,000 years cal BP. *Radiocarbon* 51(4):1111–1150.

Telford, R. J., E. Heegaard, and H. J. B. Birks, 2004, *The Holocene* 14(2):296-298.

PaleoResearch Institute
2675 Youngfield Street, Golden, CO 80401
(303) 277-9848 • Fax (303) 462-2700
www.paleoresearch.com

FIGURE 4. PRI RADIOCARBON AGE CALIBRATION

Laboratory Number: PRI-13-046-KC3-R6
Sample Identification: Microcharcoal
Conventional AMS ^{14}C Date: 329 ± 22 RCYBP
1-sigma Calibrated Age Range (68.2%): AD 1510-1640
2-sigma Calibrated Age Range (95.4%): AD 1480-1650
$*^{13}C$ ($^{o}/_{oo}$): -24.7 (Measured for ^{14}C calculation, not valid for dietary or paleoenvironmental interpretations)

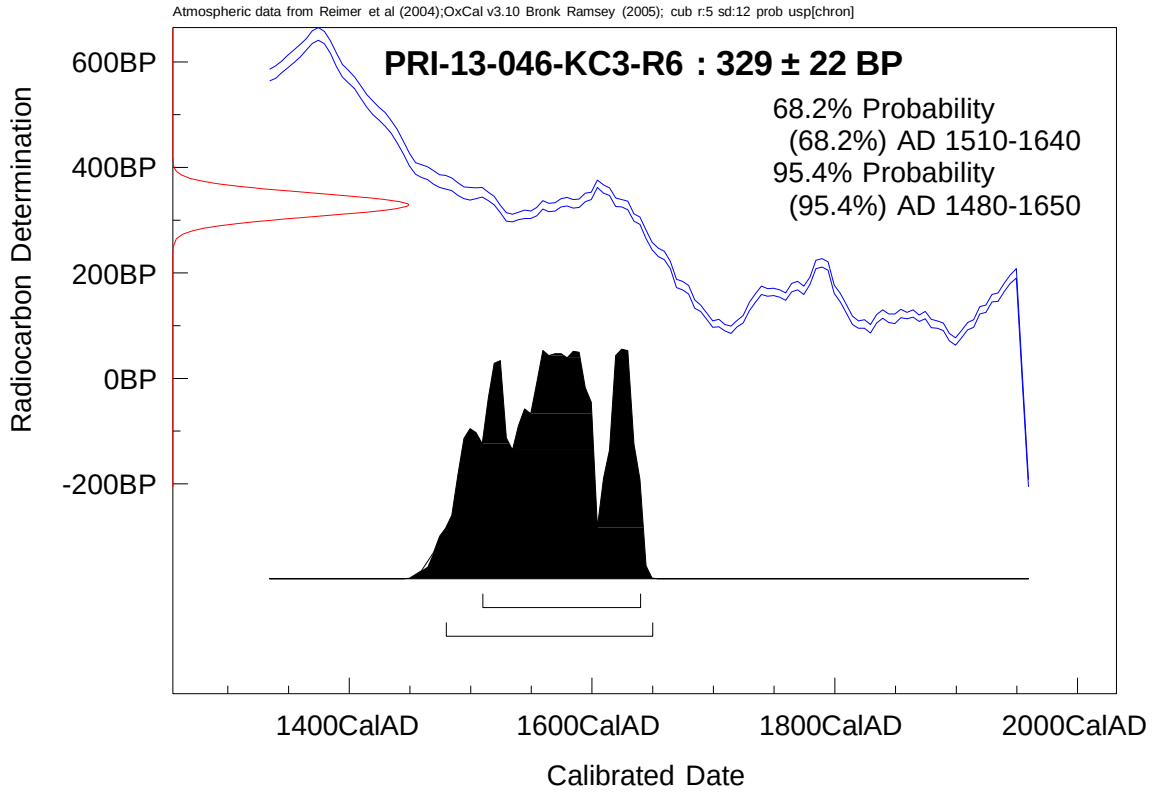

Intercept Statement. For radiocarbon calibration, PRI uses OxCal3.10 (Bronk Ramsey 2005), which is a probability-based method for converting ages in radiocarbon years (RCYBP) into calibrated dates (CAL yr BP). This method is preferred over the intercept-based alternative because instead of providing individual point estimates, it reflects the probability of the date's occurrence within a given range (reflected by the amplitude [height] of the curve). As a result, the probability-based method produces more stable calibrated values than do intercept-based methods (Telford 2004). Ongoing refinements and adjustments to the calibration curve have a greater apparent effect on individual points than on ranges.

References

Bronk Ramsey, C., 2005, OxCal. 3.1 ed. www.rlaha.ox.ac.uk/oxcal/oxcal.htm.

Reimer, P. J., M. G. L. Baillie, E. Bard, A. Bayliss, J. W. Beck, P.G. Blackwell, C. Bronk Ramsey, C. E. Buck, G. S. Burr, R. L. Edwards, M. Friedrich, P. M. Grootes, T. P. Guilderson, I. Hajdas, T. J. Heaton, A. G. Hogg, K. A. Hughen, K. F. Kaiser, B. Kromer, F. G. McCormac, S. W. Manning, R. W. Reimer, D. A. Richards, J. R. Southon, S. Talamo, C. S. M. Turney, J. van der Plicht, C. E. Weyhenmeyer. 2009. IntCal09 and Marine09 radiocarbon age calibration curves, 0-50,000 years cal BP. *Radiocarbon* 51(4):1111–1150.

Telford, R. J., E. Heegaard, and H. J. B. Birks, 2004, *The Holocene* 14(2):296-298.

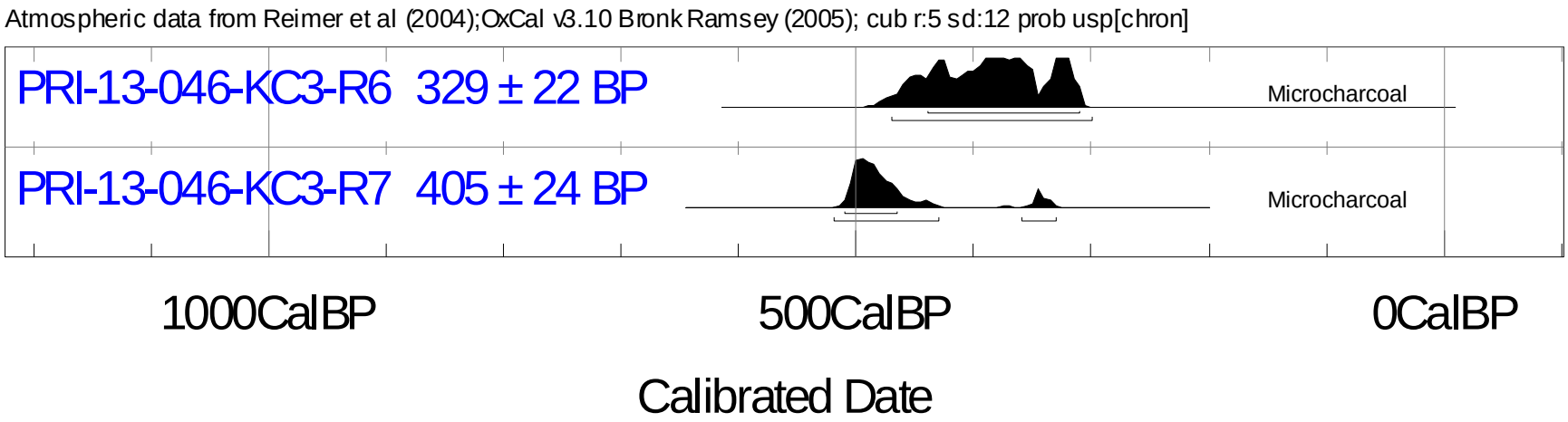

FIGURE 5. MULTIPLOT OF AMS RESULTS FOR SAMPLES FROM THE KINGS CANYON FAULT 2012 TRENCHING SITE, NEVADA.

REFERENCES CITED

Bronk Ramsey, Christopher
2005 OxCal. 3.1 ed. www.rlaha.ox.ac.uk/oxcal/oxcal.htm.

Carlquist, Sherwin
2001 *Comparative Wood Anatomy: Systematic, Ecological, and Evolutionary Aspects of Dicotyledon Wood*. Springer Series in Wood Science. Springer, Berlin.

Gulliksen, S., and E. M. Scott
1995 Report of the TIRI Workshop. The 15th International Radiocarbon Conference. *Radiocarbon* 37.

Hather, Jon G.
2000 *Archaeological Parenchyma*. Archetype Publications Ltd., London.

Hoadley, Bruce
1990 *Identifying Wood: Accurate Results with Simple Tools*. The Taunton Press, Inc., Newtown, Connecticut.

Martin, Alexander C., and William D. Barkley
1961 *Seed Identification Manual*. University of California, Berkeley.

Matthews, Meredith H.
1979 Soil Sample Analysis of 5MT2148: Dominguez Ruin, Dolores, Colorado. Appendix B. In *The Dominguez Ruin: A McElmo Phase Pueblo in Southwestern Colorado*, edited by Alan D. Reed. Bureau of Land Management Cultural Resource Series. vol. 7. Bureau of Land Management, Denver, Colorado.

Mauseth, James D.
1988 Parenchyma. Chapter 3. In *Plant Anatomy*, pp. 43-51. The Benjamin/Cummings Publishing Company, Inc., Menlo Park, California.

Musil, Albina F.
1963 *Identification of Crop and Weed Seeds*. Agricultural Handbook no. 219. U.S. Department of Agriculture, Washington D.C.

Panshin, A. J., and Carl De Zeeuw
1980 *Textbook of Wood Technology*. McGraw-Hill Book, Co., New York.

Puseman, Kathryn
2009 Choose Your Wood Wisely: Bigger Isn't Always Better. Paper presented at the Ninth Biennial Rocky Mountain Anthropological Conference, Western State College of Colorado, Gunnison.

Reimer, P. J., M. G. L. Baillie, E. Bard, A. Bayliss, J. W. Beck, P. G. Blackwell, C. Bronk Ramsey, C. E. Buck, G. S. Burr, R. L. Edwards, M. Friedrich, P. M. Grootes, T. P. Guilderson, I. Hajdas, T. J. Heaton, A. G. Hogg, K. A. Hughen, K. F. Kaiser, B. Kromer, F. G. McCormac, S. W. Manning, R. W. Reimer, D. A. Richards, J. R. Southon, S. Talamo, C. S. M. Turney, J. Van Der Plicht, and C. E. Weyhenmeyer
2009 IntCal09 and Marine09 Radiocarbon Age Calibration Curves, 0-50,000 Years Cal BP. *Radiocarbon* 51(4):1111-1150.

Schopmeyer, C. S.
1974 *Seeds of Woody Plants in the United States*. Agricultural Handbook No. 450. United States Department of Agriculture, Washington, D.C.

Taylor, R. E.
1987 *Radiocarbon Dating: An Archaeological Perspective*. Academic Press, Inc., Orlando.

Telford, Richard J., E. Heegaard, and H. J. B. Birks
2004 The Intercept is a Poor Estimate of a Calibrated Radiocarbon Age. *The Holocene* 14(2):296-298.

Kings Canyon Fault Zone

Trench 3 — West Wall

Logged by: Craig dePolo
Eric Hubbard
Anthony Crone
Ryan Gold

SE **NW**

Trench Orientation 335°

Sample No.	Unit Dated	Raw Lab Age(ybp)	OxCal Age (cal ybp)	Comments
KC3-L1	alluvial fan	5310 ±290	5300 ±300	
KC3-L2	alluvial fan	4840 ±420	4800 ±400	
KC3-L3	unit 4	3120 ±180	3100 ±200	
KC3-L4	colluvium 4	1920 ±60	1900 ±100	
KC3-L5	colluvium 3	1680 ±70	1700 ±100	
KC3-L6	colluvium 2	1660 ±80	1600 ±100	
KC3-L7	colluvium 1	1440 ±50	1400 ±100	
KC3-R1	colluvium 2	1630 ±25	1610-1410	
KC3-R2	colluvium 1	855 ±25	900-690	
KC3-R3	colluvium 1	1550 ±40	1540-1350	
KC3-R4	colluvium 2	1450 ±55	1520-1280	
KC3-R5	colluvium 2	4430 ±40	5280-4870	detrital
KC3-R6	colluvium 4	329 ±22		microcharcoal
KC3-R7	colluvium 3	405 ±24		microcharcoal

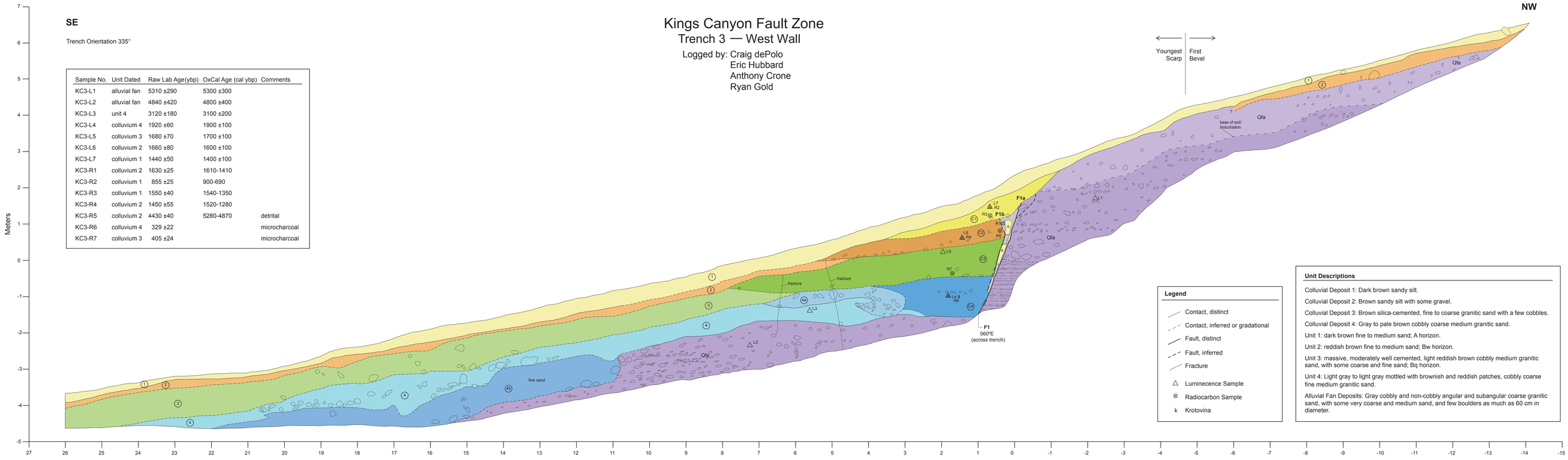

Legend

- Contact, distinct
- Contact, inferred or gradational
- Fault, distinct
- Fault, inferred
- Fracture
- Luminecence Sample
- Radiocarbon Sample
- k Krotovina

Unit Descriptions

Colluvial Deposit 1: Dark brown sandy silt.

Colluvial Deposit 2: Brown sandy silt with some gravel.

Colluvial Deposit 3: Brown silica-cemented, fine to coarse granitic sand with a few cobbles.

Colluvial Deposit 4: Gray to pale brown cobbly coarse medium granitic sand.

Unit 1: dark brown fine to medium sand; A horizon.

Unit 2: reddish brown fine to medium sand; Bw horizon.

Unit 3: massive, moderately well cemented, light reddish brown cobbly medium granitic sand, with some coarse and fine sand; Bq horizon.

Unit 4: Light gray to light gray mottled with brownish and reddish patches, cobbly coarse fine medium granitic sand.

Alluvial Fan Deposits: Gray cobbly and non-cobbly angular and subangular coarse granitic sand, with some very coarse and medium sand, and few boulders as much as 60 cm in diameter.

Kings Canyon Fault Zone

Trench 2 — South Wall

Logged by: Craig dePolo
Alexander Morelan

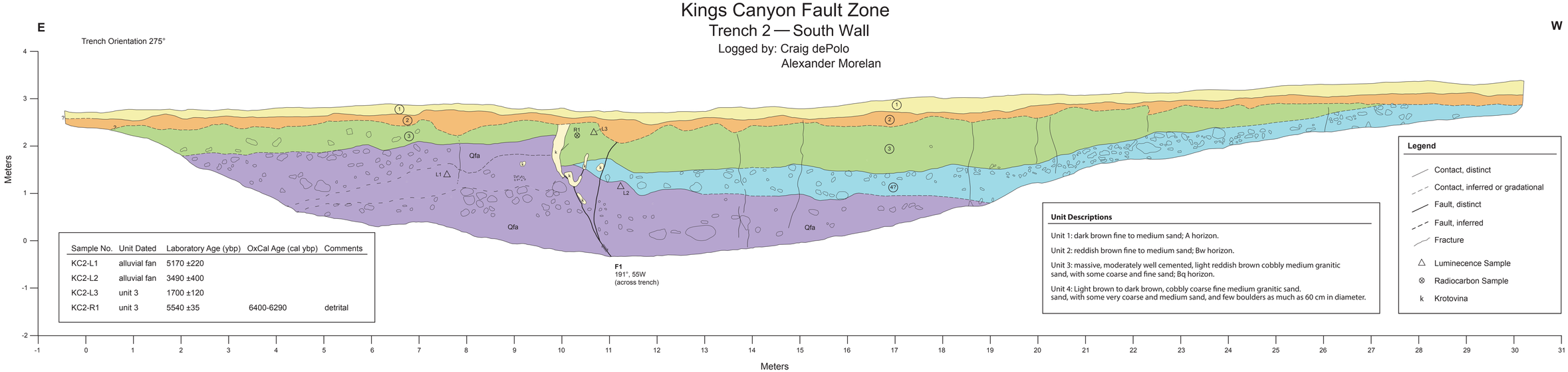

Sample No.	Unit Dated	Laboratory Age (ybp)	OxCal Age (cal ybp)	Comments
KC2-L1	alluvial fan	5170 ±220		
KC2-L2	alluvial fan	3490 ±400		
KC2-L3	unit 3	1700 ±120		
KC2-R1	unit 3	5540 ±35	6400-6290	detrital

Unit Descriptions

Unit 1: dark brown fine to medium sand; A horizon.

Unit 2: reddish brown fine to medium sand; Bw horizon.

Unit 3: massive, moderately well cemented, light reddish brown cobbly medium granitic sand, with some coarse and fine sand; Bq horizon.

Unit 4: Light brown to dark brown, cobbly coarse fine medium granitic sand. sand, with some very coarse and medium sand, and few boulders as much as 60 cm in diameter.

Legend

- Contact, distinct
- Contact, inferred or gradational
- Fault, distinct
- Fault, inferred
- Fracture
- △ Luminecence Sample
- ⊗ Radiocarbon Sample
- k Krotovina

Kings Canyon Fault

Trench 1 — South Wall

Logged by: Shaopeng Dong
Craig dePolo

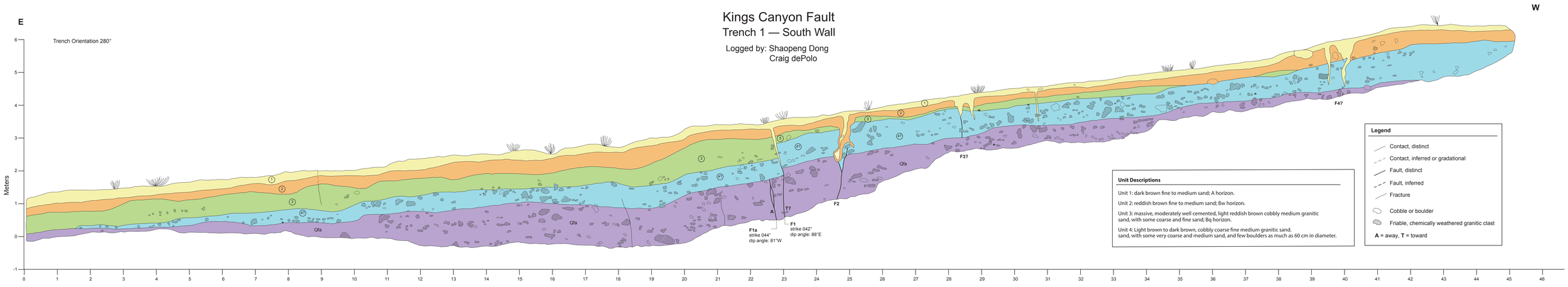

Unit Descriptions

Unit 1: dark brown fine to medium sand; A horizon.

Unit 2: reddish brown fine to medium sand; Bw horizon.

Unit 3: massive, moderately well cemented, light reddish brown cobbly medium granitic sand, with some coarse and fine sand; Bq horizon.

Unit 4: Light brown to dark brown, cobbly coarse fine medium granitic sand, sand, with some very coarse and medium sand, and few boulders as much as 60 cm in diameter.